

Clemson University

TigerPrints

All Theses

Theses

December 2021

Impact of Non Torque Loading on Wind Turbine High Speed Shaft Bearing Failure Modes During a Grid Interruption Event

Joseph Scott Roulier

Clemson University, Joeyroulier1@gmail.com

Follow this and additional works at: https://tigerprints.clemson.edu/all_theses

Recommended Citation

Roulier, Joseph Scott, "Impact of Non Torque Loading on Wind Turbine High Speed Shaft Bearing Failure Modes During a Grid Interruption Event" (2021). *All Theses*. 3634.

https://tigerprints.clemson.edu/all_theses/3634

This Thesis is brought to you for free and open access by the Theses at TigerPrints. It has been accepted for inclusion in All Theses by an authorized administrator of TigerPrints. For more information, please contact kokeefe@clemson.edu.

IMPACT OF NON TORQUE LOADING ON WIND TURBINE HIGH
SPEED SHAFT BEARING FAILURE MODES DURING A GRID
INTERRUPTION EVENT

A Thesis
Presented to
the Graduate School of
Clemson University

In Partial Fulfillment
of the Requirements for the Degree
Master of Science
Mechanical Engineering

by
Joseph Scott Roulier
December 2021

Accepted by:
Dr. Phanindra Tallapragada, Committee Chair
Dr. Amin Bibo
Dr. Richard Figliola
Dr. Shyam Panyam

Abstract

As the wind energy field continues to grow, reducing component failures will be of top priority to reducing the cost of power production. The high speed shaft (HSS) bearings are one of the leading causes of failure in wind turbines, if improvements in the operating life of turbines are to be made HSS bearing failure is one area with large growth potential. In industry, engineers use modeling and simulation techniques to better understand the potential failure modes of the turbine. Utilizing these models, turbine manufacturers can improve designs and implement control strategies to eliminate failure modes and extend the operating life of the turbine. Some of the worst loading conditions in a turbine are produced as a result of electrical events in the generator, this coupling of mechanical and electrical systems is often referred to as electromechanical interaction and is one of the leading areas of study in wind turbines. Understanding how NTL impacts HSS bearing failure modes during grid interruption events can lead to reductions in turbine failures and improvement in turbine availability. This will be studied through the use of multi-body dynamic models developed to replicate the loading in wind turbine drivetrains. Electromechanical interaction in a wind turbine drivetrain is typically studied using dynamic models of 3 distinct types. High fidelity full gearbox models, simplified torsional gearbox models, and isolated component lumped parameter models.

The first objective of this work is to outline the benefits and drawbacks of each model type and determine the appropriate model for studying the effect of non-torque loading (NTL) on high speed shaft (HSS) bearing failure modes during a transient electrical event. It was determined that the high fidelity full gearbox model was necessary to capture all the effects NTL could present in the HSS bearing failure modes. With the appropriate model selected, analysis was then performed to determine the effect of NTL on skidding and impact loading in the HSS bearings during a grid interruption event. The application of NTL in the high fidelity drivetrain model resulted in substantial differences in bearing failure modes. Applying NTL resulted in a static shift in the

bearing force away from 0, potentially alleviating concerns of skidding in the bearing during a grid interruption event. Additionally, applying NTL was seen to cause a decrease in the total impact loading seen in the bearings.

To achieve the benefits of adding NTL in the drivetrain, an offset to the generator was used to create a reaction force from the high speed shaft coupling (HSC) mimicking the NTL applied previously at the rotor connection point. This method was tested for its ability to replicate the NTL applied at the rotor and was found to do so to a high degree of accuracy. NTL was then implemented to align the HSC when the turbine is operating at full power. This new process offsets the generator to account for the torque induced misalignment in the HSC. This alignment method was shown to increase the minimal radial loading seen in each of the bearings while slightly increasing the impact loading in the 2 MW DW bearing and the 5 MW UW bearing. The minimum radial loading for the 2 MW model increased by roughly 14% and 6% of the steady state conventionally aligned radial load for the DW and UW bearings respectively. The 5 MW model saw increases of 13% and 5% in the DW and UW bearings respectively. These improvements are significant when considering the high rate of speed during the grid interruption any improvements in skidding can go a long way for the life of the turbine. Future study is needed on the potential drawbacks of the added loading but reduction in potential skidding cases could result in significant improvements in the lifespan of bearings.

Acknowledgments

I would like to express my deepest appreciation to my advisor and mentor Dr. Amin Bibo, who has spent countless hours guiding me throughout this process. I would also like to thank Dr. Shyam Panyam, for providing me additional support and invaluable insight along the way. I am exceedingly thankful for the opportunity given me to work at such an innovative facility like the Dominion Energy Innovation center where I was encouraged to grow as an engineer. The EIC provided me tremendous support throughout this process and I will always be grateful for the opportunity provided to me. I would like to thank my committee chair Dr. Tallapragada for being so accommodating throughout this process and Dr. Figliola for providing me with support and guidance, whenever possible.

Table of Contents

Title Page	i
Abstract	ii
Acknowledgments	iv
List of Tables	vii
List of Figures	viii
1 Introduction	1
1.1 Motivation	1
1.2 Previous Studies	4
1.3 Objective	5
2 Modeling Considerations for Electromechanical Interaction	6
2.1 Wind Turbine Drivetrain Components	6
2.2 Model Fidelity Considerations	9
2.3 Electromechanical Interaction Modeling Techniques	10
2.4 Drivetrain Model Descriptions	11
2.5 Investigation Strategy	17
2.6 Generator Rotational Velocity Study	20
2.7 Bearing Load Study	24
2.8 Summary	28
3 Effects of Non-Torque Loading on High Speed Shaft Bearing Failure Modes	32
3.1 Drivetrain Model Selection	32
3.2 Grid Interruption Event Description	33
3.3 Test Profile Description	33
3.4 Gear Mesh and Bearing Force Reactions	37
3.5 Bearing Failure Modes	39
3.6 Bearing Loads Under Static Non-Torque Loading	41
3.7 Summary	45
4 Effects of Generator Offset on High Speed Shaft Bearing Failure Modes	46
4.1 Application of NTL to Drivetrain	46
4.2 High Speed Shaft Coupling Alignment Considerations	48
4.3 Proposed Alignment Procedure	51
4.4 Offset Generator Bearing Response to Grid Interruption Events	53
4.5 Summary	57
5 Conclusions and Discussion	59

5.1 Future Work	60
Bibliography	61

List of Tables

2.1	Steady state generator speed frequencies captured by model configurations	21
2.2	Misaligned steady state generator speed frequencies captured by model configurations	24
2.3	Steady state UW bearing force frequencies captured by model configurations	25
2.4	Summary of model configurations	31
3.1	Grid interruption transience of 2 MW and 5 MW models with static NTL	44
4.1	2 MW model grid interruption transience for conventional and proposed alignments	57
4.2	5 MW model grid interruption transience for conventional and proposed alignments	58

List of Figures

1.1	Downtime hours accumulated from 2003 to 2007 for wind turbines operating in Germany [12]	2
1.2	Percentage of gearbox failures by component from NREL study [14]	3
2.1	Full wind turbine components [17] (top) drivetrain subsystems (bottom)	7
2.2	Three point suspension system for a wind turbine [18]	8
2.3	High speed shaft bearing locations [15]	9
2.4	High fidelity gearbox composition	14
2.5	Diagram of gear slicing [2]	14
2.6	Simplified gearbox composition	16
2.7	Isolated HSC and lumped gearbox and generator model	17
2.8	Steady state operating conditions input profiles: main shaft speed, generator torque, and bending moment used for misaligned steady state	19
2.9	Test profiles for grid interruption	19
2.10	Generator speed in steady state conditions	22
2.11	FFT of generator speed during steady state operation	22
2.12	Generator Speed during misaligned steady state case	23
2.13	FFT of misaligned generator speed	23
2.14	Generator speed for grid interruption event case	23
2.15	Time response of force in HSS DW tapered roller bearing in steady state operating conditions: axial component (left) and radial component (right)	26
2.16	Time response of radial force in HSS UW cylindrical roller bearing in steady state operating conditions	26
2.17	FFT of radial force in HSS UW cylindrical roller bearing in steady state operating conditions	27
2.18	Time response of force in HSS DW tapered roller bearing in steady state misaligned operating conditions: axial component (left) and radial component (right)	27
2.19	Time response of radial force in HSS UW cylindrical roller bearing in misaligned steady state operating conditions	29
2.20	Time response of radial force in HSS DW tapered roller bearing during a grid interruption event	29
2.21	Time response of radial force in HSS UW cylindrical roller bearing during a grid interruption event	30
3.1	Torque and speed profile of high speed and main shaft during a grid interruption event [5]	34
3.2	Diagram of HSC Misalignment	34
3.3	Time response of misalignment in the Z-direction of the high speed shaft coupling	35
3.4	Displacement of gearbox under load induces HSC misalignment [18]	36
3.5	Bending moments used to model NTL in 2 MW and 5 MW test profiles	36

3.6	Test profiles used to model grid interruption events, generator back torque (top) and rotor speed (bottom)	37
3.7	Pressure angle diagram [8]	38
3.8	Helix angle diagram (left) Helical gear free body diagram (right)	38
3.9	Free body diagram of high speed shaft [5]	39
3.10	Bearing radial force decomposition	40
3.11	Time response of 2 MW (left) and 5 MW (right) tapered roller bearing axial force during a grid interruption event	41
3.12	Time response of 2 MW (left) and 5 MW (right) tapered roller bearing radial force during a grid interruption event	42
3.13	Time response of the 2 MW (left) and 5 MW (right) cylindrical roller bearing radial force during a grid interruption event	43
3.14	2 MW bearing loading zones during a grid interruption event	44
3.15	5 MW bearing loading zones during a grid interruption event	45
4.1	Comparison of offset generator vs applied NTL on HSC Misalignment	47
4.2	Comparison of offset generator vs applied NTL on tapered roller bearing axial force during a grid interruption event	47
4.3	Comparison of offset generator vs applied NTL on cylindrical roller bearing radial force during a grid interruption event	48
4.4	Comparison of offset generator vs applied NTL on bearing loading zones during a grid interruption event	49
4.5	Rotor Weight Induced Misalignment	49
4.6	Operational misalignment of a statically aligned HSC	50
4.7	HSC Misalignment during a grid interruption event of a dynamically and statically aligned HSC	51
4.8	Procedure for dynamically aligning HSC	52
4.9	Dynamic wind profile grid interruption event set values	53
4.10	Axial loading in 2 MW (left) and 5 MW (right) DW Tapered Roller Bearing during grid interruption event of 2 alignment methods	54
4.11	Radial loading in 2 MW (left) and 5 MW (right) DW Tapered Roller Bearing during grid interruption event of 2 alignment methods	54
4.12	Radial loading in 2 MW (left) and 5 MW (right) UW Tapered Roller Bearing during grid interruption event of 2 alignment methods	55
4.13	Loading Zones in 2 MW HSS Bearings during grid interruption event of 2 alignment methods	56
4.14	Loading Zones in 5 MW HSS Bearings during grid interruption event of 2 alignment methods	57

Chapter 1

Introduction

1.1 Motivation

Wind power is one of the fastest-growing sources of new electricity supply and the largest source of new renewable power generation added in the United States since 2000. Approximately 6% of US power is currently produced by wind, with that number projected to increase to 35% by 2050 [11]. As wind turbine demand has improved so have designs, which have advanced significantly in both size and power production over the years with previous designs being rated at a few hundred kW to 15 MW turbines being deployed today. Advances in size and power production of turbines have led to an increase in the significance of component failures as downtime becomes more costly and maintenance becomes more difficult.

With the growing need for wind energy in the United States, the ability to test and accurately model wind turbine dynamics becomes even more critical. A complete understanding of wind turbine operation in the field is required to ensure accurate lifetime estimations for each of the components. Modeling events that occur in the field can help extend operating life and predict failures in various components, reducing turbine downtime. Performing tests on turbines in the field is often impossible or impractical due to the variability of weather and a lack of reproducibility in performing tests. Remote site test facilities, like the Dominion Energy Innovation Center, exist to test a wide variety of scenarios the turbine sees in operation in a controlled environment. In addition to the full-scale tests run, facilities like the Dominion Energy Innovation Center also develop and validate dynamic models of wind turbines to aid in the design and testing process.

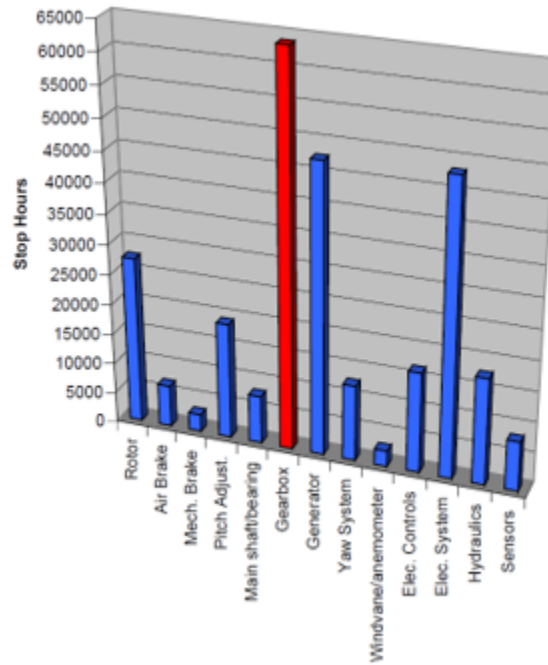


Figure 1.1: Downtime hours accumulated from 2003 to 2007 for wind turbines operating in Germany [12]

For the wind energy industry to meet its growth goals the cost of power produced by wind turbines must be reduced significantly. Compared to other conventional power production techniques wind turbines fail at a much higher rate. Few wind turbines reach their 20 year design life with most experiencing significant downtime over their years of operation. Reducing the amount of downtime a wind turbine experiences in the field is crucial to meeting the cost of power production goals for wind turbines. According to a German study, the leading cause of downtime in wind turbines comes from failures in the gearbox as shown in Figure 1.1 [12]. Most gearboxes won't last more than five years before major gearbox components, or the entire gearbox needs to be replaced. The Gearbox Reliability Database maintained by the National Renewable Energy Laboratory records that 60% of all wind turbine gearbox failures are caused by bearing failures long before the life defined by the International Organization for Standardization, and American Bearing Manufacturers Association [6].

Wind turbine manufacturers have sought to understand the leading causes of these component failures, to help improve designs and turbine performance. According to data collected by the National Renewable Energy Laboratory (NREL), approximately 47.8% of all gearbox failures come

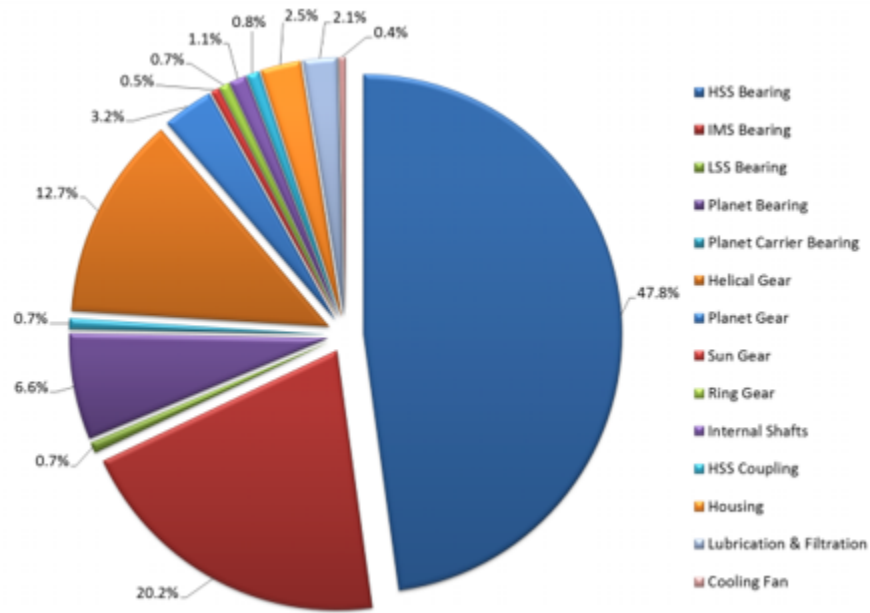


Figure 1.2: Percentage of gearbox failures by component from NREL study [14]

from the high-speed shaft (HSS) bearings and can be seen in Figure 1.2 [14]. Despite these bearings being relatively cheap to replace their failure makes up almost 28% of the total cost over the different failure modes for a wind gearbox [9]. Understanding the causes of these failures can help decrease wind turbine downtime and maintenance requirements, thus lowering the cost of energy produced by wind turbines.

Current methods to reduce failure in components like the high-speed shaft bearings are designed using simulations of the wind turbine’s behavior in various conditions. These simulations implement dynamic models to replicate the operating conditions of the turbine. Wind turbine manufacturers utilize these models to improve designs and implement control strategies to eliminate failure modes and extend the operating life of turbines. Once validated these models can run wind turbines through a large number of scenarios in many different configurations without needing to incur the cost of implementation. These models allow a more intimate understanding of the turbines to be developed as aspects are removed and changed while the impacts are observed.

One of the main reasons wind turbines fail at a higher rate than other power generation techniques is the uniqueness of the challenges they present. One factor unique to wind turbines is the coupling of electrical and mechanical components also referred to as, electromechanical interaction.

Some of the worst mechanical conditions in a wind turbine are produced as a result of electrical events. Real-world recordings of torsional load in drive systems of many different turbine models show that the worst torsional vibrations and torque reversals generally occur during transient electrical events, such as emergency stops, grid faults, and many other hard stops [4]. These transient events are recreated in simulations so an understanding can be built of how forces in the turbine change as the event occurs. Current failure data shows few wind turbines are reaching their design life with a large number seeing significant downtime during their operation. This indicates a need for further study on the accuracy of the models being used in industry to replicate these transient events and associated failure modes.

1.2 Previous Studies

As gearbox failures continue to be the dominant cause of downtime in wind turbines, the gearbox reliability collaborative (GRC) was developed by NREL and the National Wind Technology Center (NWTC) to study gearbox failures. This collaborative seeks to reveal the causes and loading conditions that result in the premature failure of wind turbine gearboxes [13]. The GRC has performed a number of studies on components inside wind turbine gearboxes with the main focus being bearing health. One such study sought to investigate high-speed shaft bearing loads through modeling and dynamometer testing [5]. This study was performed to better understand the causes of axial cracks in the high-speed shaft roller bearings of wind turbines. The study examined 4 different scenarios of turbine operation for their effect on bearing loads. These scenarios were pure torque operation, applied rotor moments, braking events, and grid loss events.

The study found a minimal impact of rotor moments (NTL) on the high-speed shaft bearing loads. It was determined that the force in the bearing due to NTL was small in comparison to the torque induced loading. This study, however, was for a small turbine with a relatively small NTL. Wind turbines in use today are much larger in size and power rating than the ones used in this study. These larger wind turbines experience much larger NTL than the ones tested in NREL's study, which have the potential to have a greater impact on the forces in the bearing. This study found that severe transient events produced loading conditions deemed detrimental to the life of the bearing. With transient events like grid interruptions being one of the potential leading causes of failure in HSS bearings.

1.3 Objective

The main goal of this work is to determine the effect NTL has on bearing failure modes during a grid interruption event. This work will first outline the appropriate drivetrain model to implement for various electromechanical analyses, and which model is the most suitable for studying bearing failure during grid interruption events. Next, the impact of NTL on the potential failure modes of HSS bearings during grid interruption events will be studied. Specifically, from the mechanical perspective, the HSS bearings will be investigated for the impact NTL has on skidding and impact loads seen in the bearings. After determining the impact NTL has on the bearing failure modes potential improvements to the drivetrain configuration will be recommended. A new alignment method for the HSC will be proposed with the goal of increasing the life of the HSS bearings by reducing behavior commonly associated with failure in the bearings. This new alignment method will then be simulated to test for its potential benefit in comparison to the conventional HSC alignment procedure.

Chapter 2

Modeling Considerations for Electromechanical Interaction

2.1 Wind Turbine Drivetrain Components

Before the impact of NTL on HSS bearing failure can be studied, the wind turbine drivetrain must first be understood. Drivetrains contain all the main components of the wind turbine seen in figure 2.1, except for the blades, hub, and tower. The drivetrain consists of all the components necessary to convert the mechanical energy of the wind to electrical energy supplied to the grid. There are 5 main components that make up a typical horizontal axis wind turbine (HAWT) drivetrain and are shown in figure 2.1. These components are the bedplate, main shaft, gearbox, high-speed shaft coupling (HSC), and generator. Each of these components can be found inside the outer metal housing often referred to as the nacelle.

The main shaft is the primary interface of the rotor to the drivetrain. The main shaft transmits all the forces generated by the rotor to the drivetrain. These forces come in the form of torque, which drives rotation, and non-torque loading (NTL), which does not. This NTL is primarily made up of the weight of the rotor as well as the axial forces and bending moments from uneven wind loading. The loading generated by the rotor of a multi-megawatt wind turbine can be very large in magnitude and as a result, the turbines in this analysis utilize a 3 point suspension system to isolate the drivetrain components from the loading created by the rotor. The suspension gets its

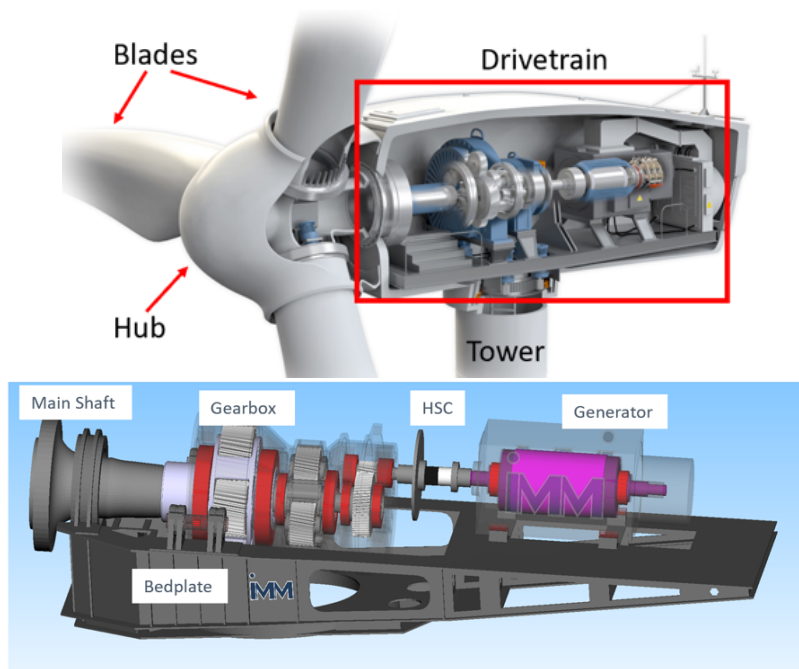


Figure 2.1: Full wind turbine components [17] (top) drivetrain subsystems (bottom)

name from the 3 points of connection from the drivetrain to the bedplate, 1 main bearing, and 2 compliant torque arms as seen in figure 2.2. The main bearing is designed to be very stiff and is used to react most of the NTL from the main shaft into the bedplate and through the tower. The goal of this main bearing is to isolate the loading in the drivetrain from the extreme NTL seen in the main shaft. The main shaft can also be viewed as the input shaft into the gearbox where it interfaces with the first stage planet carrier.

The gearbox used in this analysis is a three-stage planetary gearbox that allows the high torque low velocity rotations created by the rotor to be stepped up to a speed that is usable for power production in the generator. The gears present in the turbines modeled are helical gears, which are used to increase the number of gear teeth in mesh, as well as reduce noise from the high speeds in the turbine drivetrain. Each gear is fixed to a shaft using support bushings and each shaft fixed to the housing using 2 bearings. There are 3 shafts present in the gearbox: the main shaft, the intermediate shaft (IMS), and the high speed shaft (HSS). The gearbox housing is fixed to the bedplate using 2 compliant torque arm mounts that help damp torsional vibrations from the system as well as react loading from the torque transmission throughout the drivetrain. The torque arms

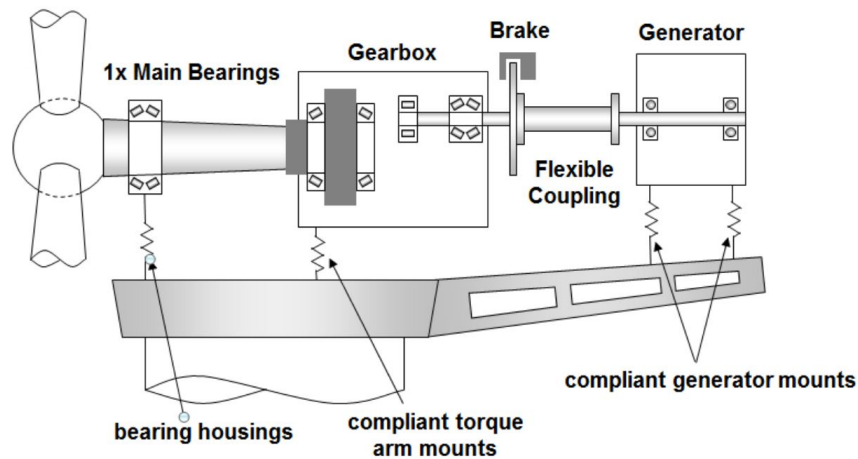


Figure 2.2: Three point suspension system for a wind turbine [18]

provide an axial and radial force to react the torque transmission in the drivetrain.

The high speed shaft (HSS) is the output shaft of the gearbox and is connected to the generator by the high speed shaft coupling (HSC). The HSS has 2 support bearings that attach the shaft to the housing and prevent movement of the shaft. These bearings are referred to by their location in the turbine using upwind (UW) and downwind (DW) as the naming convention. The bearing's location on the shaft can be seen in figure 2.3. The bearing in the upwind position is used to model a cylindrical roller bearing (CRB) that only provides reaction forces in the radial direction. The downwind bearing is a back-to-back tapered roller bearing pair (TRB) that supports the shaft by providing forces in the axial and radial directions.

The HSC is used to transmit the mechanical power supplied from the gearbox to the rotor of the generator. Most generators take the rotational velocity of the rotor and pass it through an electrical field generated by the stator to generate electrical power. There are a wide variety of generation constructions, used to achieve this power transmission, that go well beyond the scope of this report. However, for nearly all generator constructions to operate at their highest efficiency the rotor must have very little misalignment inside the stator. For this reason, the HSC is used to take all of the operational misalignment created in the drivetrain and still transmit a constant rotational velocity to the rotor. The HSC allows large misalignments on the gearbox side of transmission while the generator side stays nearly fixed. In addition to this very important purpose, the HSC in modern wind turbines also provides a torque limiting function where large torques are not transmitted to

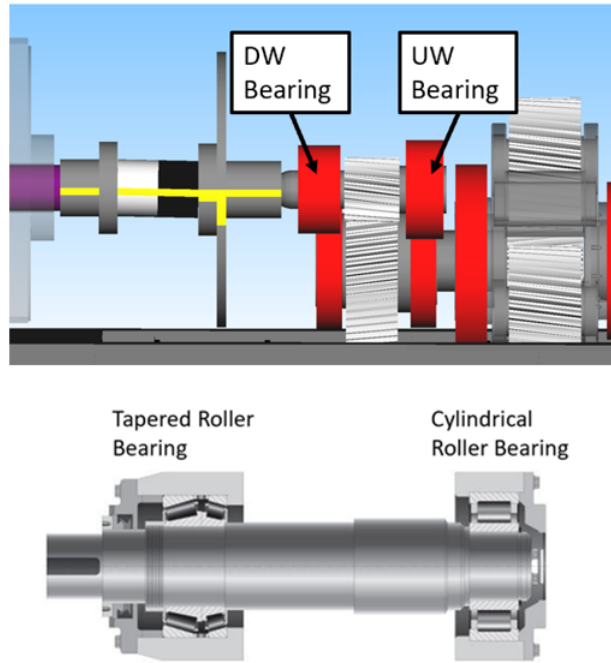


Figure 2.3: High speed shaft bearing locations [15]

the gearbox from the generator and are instead "slipped". The torque limitation prevents damage to gearbox components during severe electrical events like grid interruptions and generator short circuits that might produce damaging torques in the gearbox [3].

The bedplate is a steel structural frame meant to provide a rigid support for the components to mount to. The frame allows for all of the components to be rotated together when the turbine changes direction to face the wind. The bedplate reacts the NTL seen in the main shaft through the main bearing and the torque transmission in the drive train through the torque arms. The bedplate is also connected to the generator through stiff bushings meant to isolate the generator movement from the rest of the drivetrain. The bedplate is then connected to the tower through the YAW bearing which allows both the nacelle and rotor to be rotated to face the wind.

2.2 Model Fidelity Considerations

Model fidelity is a concept used to describe the relative complexity of a model. Fidelity for multi-body dynamic models, such as this one, is generally increased by adding degrees of freedom

and flexibility to the components. By adding these degrees of freedom new stiffness and damping components must also be defined. The added degrees of freedom also severely slow the computation time of the model. The higher fidelity the model the more accurately the model represents the real world. Often engineers are tasked with making trade-offs between model fidelity and computation times for their applications. By understanding the model fidelity necessary for each study, simulations can be performed quicker, and products developed faster. Consequently, removing degrees of freedom of components and making bodies rigid can greatly decrease computation time and simplify results, but will lead to aspects of the simulation being removed or becoming inaccurate. Deciding where simplifications can be made is one of the key responsibilities of modeling engineers.

When modeling complex systems, like wind turbines, simplifications must often be made to reduce computation times and simplify analysis. Full turbine models are incredibly complex and often require information that even component manufacturers do not know. Maintaining these complex models with up to date information can be costly and time consuming. Instead, analysis is normally performed modularly, with each component owner developing models specific to their component. This can often cause a disconnect in the design process where full systems are not tested together until the final stages of the design process causing widespread changes to be made at the end of the design process. By better understanding the capabilities and limitations of each of these reduced models, designs can be improved before reaching the final stages of the development process. Two previous studies by Matzke [1] and [10] were performed to validate wind turbine models for their ability to replicate bearing and gear tooth loads inside a wind turbine gearbox. The studies focused on determining what model parameters influence calculation objectives and fidelity requirements to produce meaningful results.

2.3 Electromechanical Interaction Modeling Techniques

When simulating wind turbine dynamics there are a wide variety of modeling techniques used to capture the behavior of the wind turbine. Most of these approaches fall into 3 distinct categories: high fidelity full system models, simplified torsional models, and lumped parameter isolated component models. Each of these model types are built with a specific purpose in mind. The high fidelity full system model is meant for highly detailed analysis on individual components or analysis requiring the highest accuracy of results. These models are rarely used in industry as the

models can be incredibly complex and difficult to use. Additionally, simulations can take significant computation efforts often taking hours to simulate a short period of operation. Keeping these models up to date can be difficult as design changes are constantly being made by component designers and implementing the changes to these complex models can be difficult.

Since the behavior of the turbine is often needed over a wide array of conditions, in most cases, running the high fidelity models would significantly slow down the design process. Instead simplified torsional models are used as they reduce the number of degrees of freedom significantly and in some cases upper bound the loading in components by making connections rigid. These models are widely utilized in industry as they are easy to maintain and designed to be run quickly in a wide variety of configurations. In most applications, these reduced fidelity full system models are utilized to generate forces and states at critical component interface points, which in turn can be used as inputs to isolated component models. These models focus on the torsional degrees of freedom as they often are the primary source of loading and analysis.

Isolated component models are used to run individual components through a wide variety of scenarios faced by a wind turbine without needing the computation efforts of a more complete system model. These models can be extremely detailed for the components of interest but simplifications of the interfaces allow for fast computations. These models are built by lumping the parameters of the full size models into single elements at the boundary conditions. With the reductions, a wide array of analyses can be conducted quickly with minimal knowledge of the other components in the turbine. This allows for modular designs to be tested without needing to perform full system analysis. In this study, each of these models will be built for the purpose of studying the electromechanical interaction in the turbine. These models will then be investigated for their appropriate uses and an appropriate model chosen for an investigation of HSS bearing failure modes.

2.4 Drivetrain Model Descriptions

SIMPACK is a commercial multi-body simulation software used in many different industries to simulate complex mechanical systems. It is often used in the wind industry to describe and predict motion and forces inside a turbine. It models gears, bearings, and other components using springs and dampers. It also captures structural deformation of flexible bodies using the Craig-Bampton method. SIMPACK generates the equations of motion for a multi-body dynamic system utilizing

non-linear second order systems of ordinary differential equations (ODEs). SIMPACK will be used in this study to build models of each of the 3 fidelity levels previously described and perform an analysis on the electromechanical interaction in the drivetrain. Each of the models were developed with assistance from researchers at the Dominion Energy Innovation center. The models contained in this section were all adapted to meet the needs of this study from a 5 MW reference model provided by NREL as a benchmark in the industry.

Before describing the key differences across model configurations, the aspects of the drivetrain models in common will be identified. The first common component is the generator. The generator in each of these models were built to only capture the mechanical effects in the turbine. This means the power electronics are not considered in the model and instead a single torque signal is used to lump the dynamics of the generator into a single element. This torque can be used to model complex electrical events for their mechanical impacts in the turbine. In some turbine generators this torque is controlled to maintain constant power output from the turbine at the rated power. However there are many different generator configurations that all achieve constant power production in unique ways. Lumping the electronics in this model allows for a wide array of generator configurations to be tested without a strong understanding of how to model each type. This torque signal is used to model the complex electrical portion of the generator in each of the 3 models.

In these models the rotational velocity of the input shaft is achieved by using a PI speed controller supplying torque at the rotor connection point to achieve a reference input speed profile. This controller is meant to achieve the desired rotational velocity in the main shaft, without losing the dynamics of the rotor. This simplification removes the complex dynamics of 3 flexible blades and aerodynamic interaction that drives rotation. Since this study is only about drivetrain considerations it is suitable to instead lump the inertia of the blades and use a controller to replicate the dynamics of the blades. Utilizing, each of these modeling techniques common to the 3 different models, testing conditions were specified for the simulations.

2.4.1 High Fidelity Full Drivetrain

The main aspect of the high fidelity model that makes it unique is the gearbox. As reductions in other drivetrain components yield little improvements in computation time and complexity, the gearbox was the only aspect changed across the two highest fidelity levels. The gearbox used in the high fidelity full drivetrain model is a 3 stage planetary gearbox containing the full contact geometry

of the gears shown in figure 2.4. The force elements used to capture the transmission forces in the gears are extremely complex and capture large amounts of information about the torque transmission in the gearbox. The model requires a deep understanding of the gearing inside the wind turbine to be constructed. Building the model can be incredibly time consuming and difficult as most of the information required is proprietary and not made readily available by the gearbox manufacturers. There are a wide variety of modeling considerations that must be made to capture the desired behavior in the gearbox. As the models used contain the proprietary information of the turbine manufacturer, individual modeling considerations will not be presented instead a few key aspects the model accounts for are identified.

One of the key aspects of the gear meshing captured in the high fidelity model is individual tooth contact. The individual contact of gear teeth allows for meshing frequencies to be present in the drivetrain. Additionally, individual gear tooth slicing is captured in the model, as shown in figure 2.5. This gear slicing allows the model to capture the effects of misalignment in the drivetrain as the gear tooth is discretized into slices over the overlapping width of the gear mesh. Each slice has an input stiffness and damping value that governs the resulting forces generated during transmission. The model also accounts for gear teeth flank modification effects due to extreme loadings that change the shape of gear teeth. This allows the full effects of severe load cases to be seen in the drivetrain and accurate stresses to be represented in the teeth. The model also uses helical gears to transfer torque through the gear box which requires defined helix and pressure angles. These angles causes the torque transmission to produce reaction forces in the shaft in non torque directions. These angles capture the misalignment and bearing loads induced in the drivetrain from torque transmission. In addition to the contact geometry this model also captures the support bushings for all the gears and bearings for each of the shafts in the drivetrain. These support bushings and bearings allow misalignment in the drivetrain and ensures the correct load path through the drivetrain.

Modeling the gearbox with this level of precision is often necessary to understand the spectrum of frequencies excited in the gearbox, as well as performing detailed analysis on the gears. This model can be utilized to study the impact of various mechanical frequencies on the electrical components in the generator. This model can also be used to perform detailed component analysis during severe electrical events. High fidelity models like this one can be incredibly computation heavy taking long periods of time to run simulations with large amounts of information being required to produce accurate results. In this study the high fidelity full gearbox model contains 325 degrees

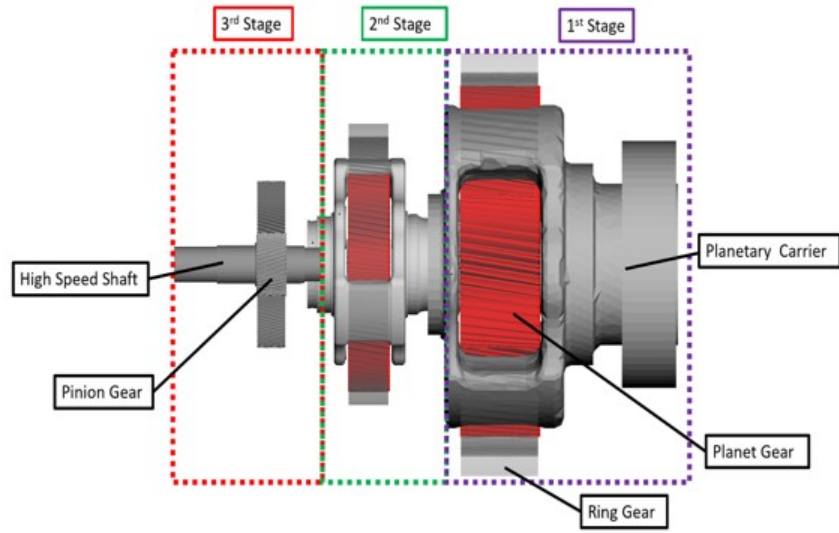


Figure 2.4: High fidelity gearbox composition

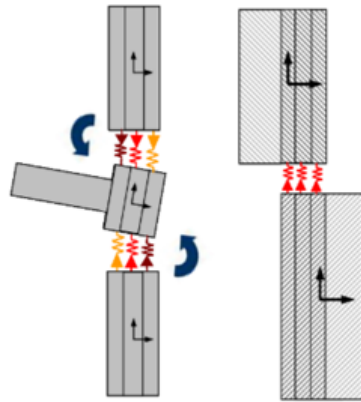


Figure 2.5: Diagram of gear slicing [2]

of freedom and a 50 second steady state operation simulation takes 34 minutes and 20 seconds to complete. To better capture the computation efforts required a time factor can be calculated (TF) which is defined in equation 2.1.

$$TF = \frac{Computation\ Time}{Simulation\ Time} \quad (2.1)$$

The time factor for the high fidelity model was calculated to be 41.24. These extensive computation efforts make these models less than ideal for most wind turbine simulation applications. Additionally, wind turbine gearboxes are normally developed by external companies, that often seek to keep designs confidential. This makes generating complex gearbox models for use in full system models difficult or even impossible. Instead turbine manufacturers utilize simplified models when possible.

2.4.2 Simplified Torsional Gearbox Drivetrain

To reduce computation times and model complexity, simplifications in the models are often made. In this instance the gearbox is simplified by removing the complex gear geometry and instead lumping each gear into a single inertia element connected rigidly to the shafts and carriers. Removing the gear and shaft support bushings significantly reduces the complexity of the drivetrain and allows for many of the calculations to be simplified. This model still distributes the inertia throughout the gearbox but does not allow for any misalignments possibly changing the load path through the drivetrain. A diagram of this simplified model can be seen in figure 2.6. Forces used to represent support bearings and bushings are calculated through the joint forces required to keep these connections rigid. This in a way provides a conservative estimation of the forces seen in the support bearings as in reality the deflection of bearings will allow for some of the loading to be reduced.

The gear meshing is considered only by relating the velocity of the different stages in the gearbox. The forces between gears are not generated instead a torque to torque relation is used between the input and output shafts of each stage. Modeling the gearbox in this way allows for the full torsional analysis of the gearbox without all the detailed forces generated by the bushings and gear meshing. Engineers use models like this one when investigating overall nacelle behavior instead of individual gearbox analysis. These models are often utilized when designing control systems and performing torsional analysis. Turbine performance is dominated by its torsional

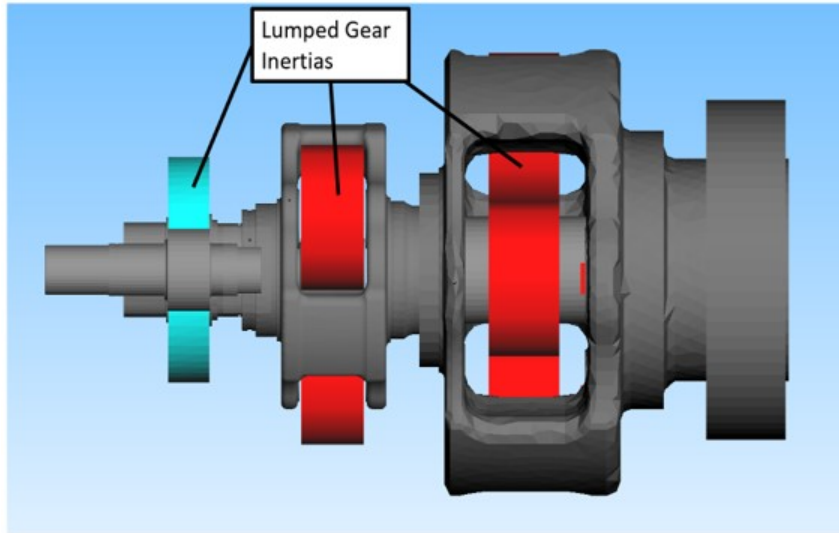


Figure 2.6: Simplified gearbox composition

dynamics and, as a result, only the torsional aspects of the model are considered in most system level applications. These reductions speed up the computation times of the drivetrain model significantly as the degrees of freedom are reduced to 205 and the time factor was calculated to be 8.76. The same simplifications used in this model are often used in the full turbine models to generate loading conditions at critical interface points for individual component designs in various severe wind cases. These loading conditions are then used as inputs to lumped parameter isolated component models.

2.4.3 Lumped Gearbox and Generator Model

The final model used was an isolated high-speed shaft coupling with boundary conditions designed to represent the generator and gearbox interactions. In this model both the down wind components (generator) and upwind components (gearbox and rotor) were lumped into single inertial elements with corresponding stiffness and damping matrices. The lumped model of the upwind components is used to replicate the dynamics of the mechanical side of the electromechanical interaction under varied loading conditions simply at the high-speed shaft coupling connection point. This ignores all the complex dynamics present upwind in the turbine and instead takes only the forces seen by the high-speed shaft coupling at the connection point. The coupling can then be orientated in different manners to replicate various misalignment cases for power transmission. Rather than maintaining full drivetrain models this HSC only model can be run through a wide array of

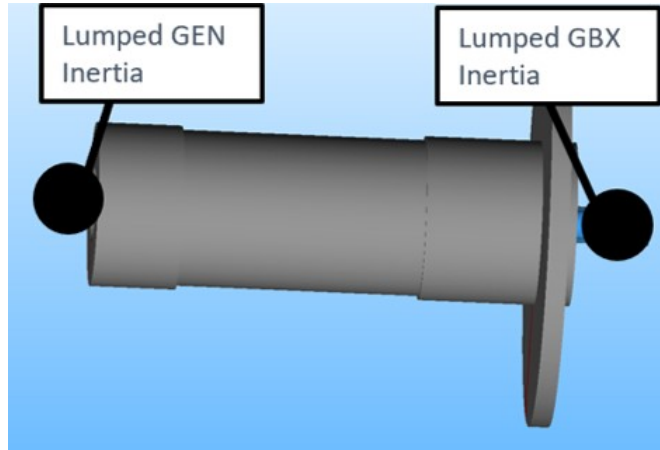


Figure 2.7: Isolated HSC and lumped gearbox and generator model

scenarios needing only to input the forces seen at the interface point once the inertial values are specified. This model significantly reduces computation time allowing very detailed models of the electrical components to be run while coupled to the mechanical system without needing to worry about computation times. The isolated HSC model used in this analysis contains only 35 degrees of freedom and the time factor was calculated to be 1.46. This model is commonly used in electrical applications as the HSC is the only mechanical component interfacing with the electrical system.

2.5 Investigation Strategy

To determine the best applications for each of the 3 models constructed, the models must be investigated for their relative ability to replicate the dynamics of the wind turbine in various operation conditions. This study will focus on comparisons of how each model captures the electromechanical interaction in the turbine. To do so 3 operating conditions are used: steady state operation, misaligned steady state operation, and a transient electrical event (grid interruption). To simplify the analysis only 2 components will be investigated. The first being the loading in the high speed shaft bearings. Representative of the mechanical portion of the electromechanical interaction the loading in the high-speed shaft bearings is of primary concern in the analysis presented in chapters 3 and 4. Focusing the investigation to these bearing loads will allow the correct model to be implemented in future analysis.

Additionally, the electrical portion of the electromechanical interaction will be investigated.

For the simplified generator model used in this report the only signal to be investigated is the rotational velocity (ω) of the generator rotor. Furthermore, the torque produced by the generator (T) is a specified input, representing the complex dynamics occurring in the generator during each operating condition. A result of this assumption is that the power generated by the turbine (P) is governed by equation 2.1. Understanding what is lost from both of these components will allow for a recommendation to be made on the appropriate model for various types of analysis.

$$P = T\omega \tag{2.2}$$

The first test profile simulated is for the wind turbine in steady state conditions. This is achieved by ramping up the speed of the main shaft and back torque of the generator as shown in figure 2.8. This test profile is used to ensure the normal operation of the turbine is replicated by each of the models and is the simplest test performed. The second profile tested was for steady state misaligned operation. This ensures that the wind turbine dynamics associated with NTL and misalignment are captured by each of the models. The input main shaft speed and generator torque profiles are the same as in figure 2.8 with the addition of a bending moment applied at the rotor connection point as shown in figure 2.8. In the lumped parameter isolated HSC model the misalignment in the HSC corresponding to that in the other models is specified as an initial condition instead. The final profile simulated is the grid interruption event. This simulation is used to ensure the drivetrain models all behave in a similar manner when a transient electrical event is applied. Most studies on electromechanical interaction focus on these severe transient events, as a result the differences in responses needs to be noted for each of the cases. For this profile the main shaft speed and generator torque profiles are shown in figure 2.9, with the loss of generator torque representing an interruption from the grid.

To determine the best model for studying the effect of NTL and misalignment on HSS bearing failure modes each model will be investigated for their relative differences. The first key difference between models is the method of representing the bearings. In the high fidelity full gearbox model, the HSS bearings are represented as lumped stiffness and damping values that exert a force between the HSS and gearbox housing. This assumes a linear relationship between displacement of the bearing and force. This is a very good approximation of the behavior of the bearing under normal

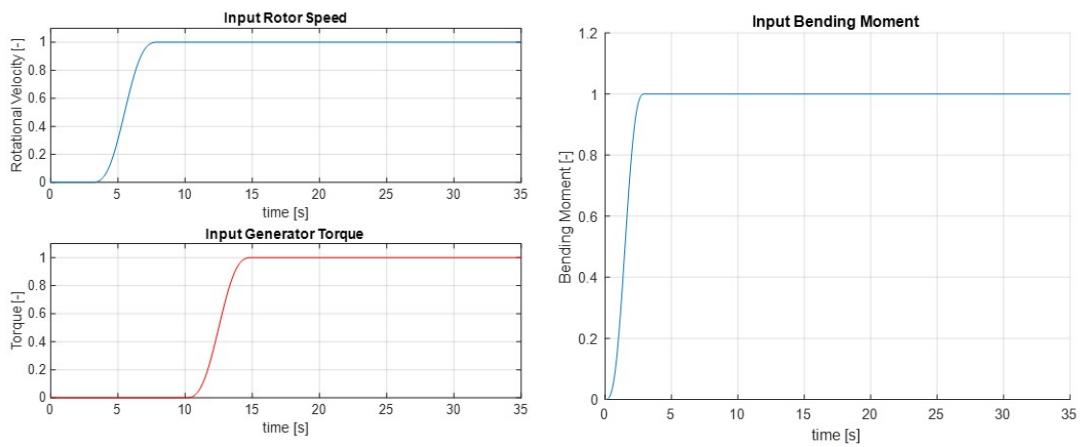


Figure 2.8: Steady state operating conditions input profiles: main shaft speed (top-left), generator torque (bottom-left), and bending moment used for misaligned steady state (right)

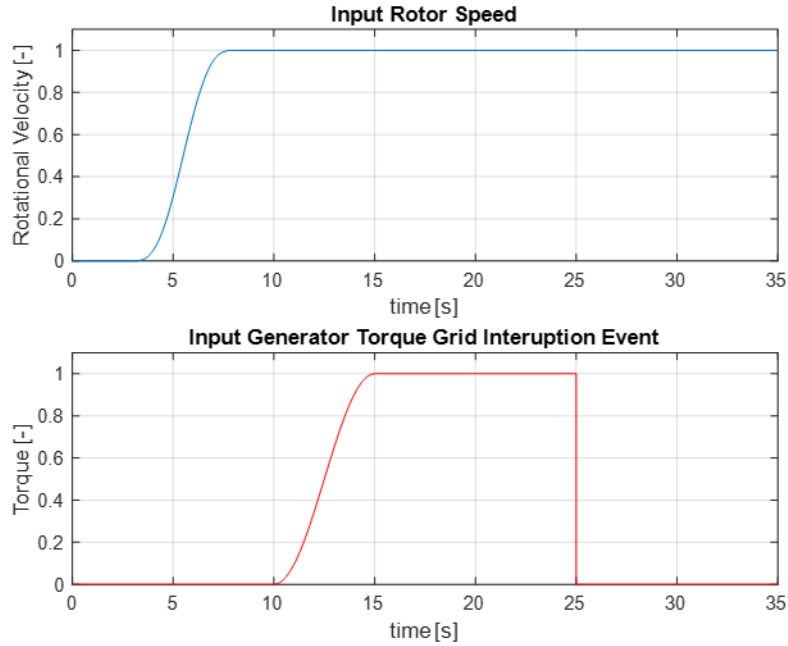


Figure 2.9: Test profiles for grid interruption

loading conditions. The bearing model used does not take into account the contact geometry of the bearing, but this information was not readily available for this analysis. In the simplified torsional model the bearing connections throughout the gearbox were modeled as simple rotational joints, thereby not permitting misalignments in the drivetrain. The force required to achieve these rigid connections is calculated and used to represent the bearing forces. In theory this assumption should upper bound the forces seen in the bearing as allowing deflection at the connection normally relieves some of the loading. This however might not be the case as neglecting misalignment can change the load path through the drivetrain.

2.6 Generator Rotational Velocity Study

2.6.1 Steady State operation

The time domain response of the rotational velocity of the generator rotor of each of the 3 models can be seen in figure 2.10. In this figure you can see that the response across the 3 models is largely unchanged. The main difference comes from the small oscillations seen in the full and simplified gearbox drivetrain models not seen in the lumped parameter model. To further investigate these oscillations a Fast-Fourier transform (FFT) was performed on the data to determine what frequency oscillations were present and their corresponding amplitude. The FFT performed is shown in figure 2.11.

While all the oscillations are small in amplitude a few significant frequencies are present in the responses. The first frequency identified at approximately 39 Hz is the 2N coupling misalignment frequency, where N represents the HSS speed in Hz. This frequency occurs at twice the rotational velocity of the HSS and is known to occur with misalignment in the HSC. The 2N frequency is present in both the full and simplified models as each model captures the torque roll induced by the compliant gearbox mounts. The reaction of torque through the drivetrain and eventually the compliant gearbox torque arm mounts allows rotation of the gearbox and as a result creates misalignment in the HSC. The misalignment in the lumped parameter model was specified to be 0 as this test case was for the turbine at steady state operation. Since the lumped parameter model does not contain the influence of torque roll the 2N frequency is not present in the response. The next two frequencies are found only in the full drivetrain model and are gear meshing frequencies. As each gear tooth makes contact, oscillations are induced in the rotational speed of the HSS. These gear meshing

Table 2.1: Steady state generator speed frequencies captured by model configurations

Model Type	2N Frequency	Gear Mesh Frequencies
Full Gearbox	X	X
Simplified Gearbox	X	
Lumped Parameter		

frequencies will only be captured by the full drivetrain model as it is the only model with the gear teeth interaction accounted for. Table 2.1 presents a summary of the frequencies captured by the different model configurations.

2.6.2 Misaligned Steady State operation

The time response with misalignment present is nearly identical to that of the steady state response and can be seen in figure 2.12. An FFT was again generated to investigate the oscillations and shown in figure 2.13. The FFT shows each of the same frequencies from the steady state model. Table 2.2 presents a a summary of the frequencies captured by the different model configurations in misaligned steady state operation. The gear mesh frequencies remain unchanged from the steady state responses. The 2N HSC misalignment frequency has increased in magnitude for each of the models. The simplified and lumped models have nearly identical amplitudes while the full gearbox is slightly larger. The full gearbox model experiences more misalignment than the simplified and lumped parameter models, as the angles captured by detailed gear geometry transfer more force and compliant support bushings allow for more displacement in the drivetrain. As a result of the added displacement, more misalignment is created in the HSC. The simplified model was built to ignore the misalignment inside the gearbox to simplify analysis, so smaller misalignment at the HSC is to be expected. The amplitude of the 2N frequency component is known to increase with increase in misalignment so these results are to be expected. Again a significant portion of the dynamics is ignored in the simplified and lumped gearbox models as the gear mesh frequencies are only captured in the full gearbox model. While there are definitive distinctions between models the overall differences in generator speeds are negligible with the amplitudes of oscillation in the speed being less than .02% of the rated speed of the generator.

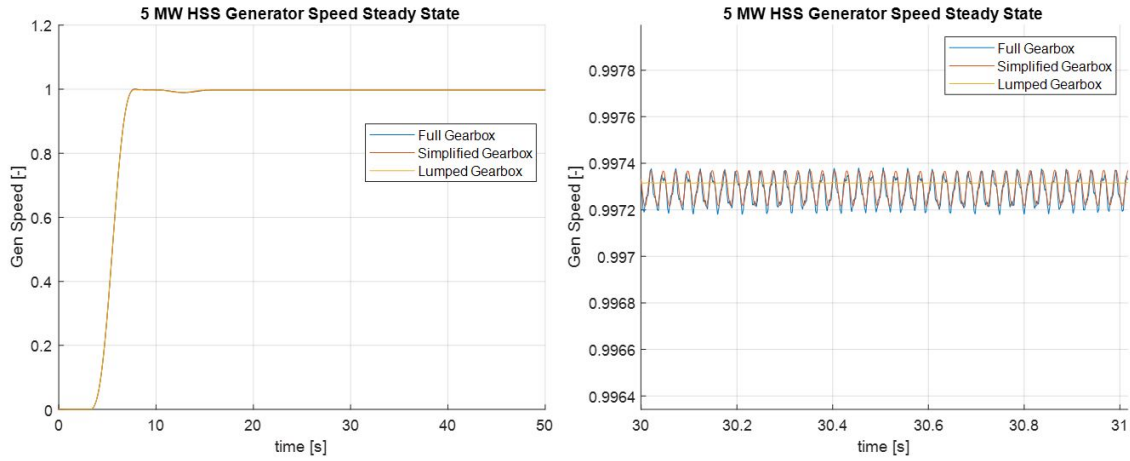


Figure 2.10: Generator speed in steady state conditions

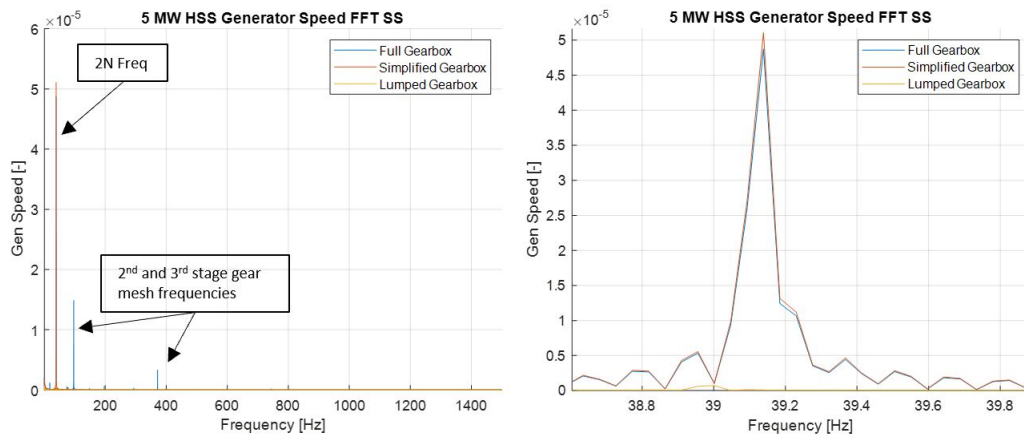


Figure 2.11: FFT of generator speed during steady state operation

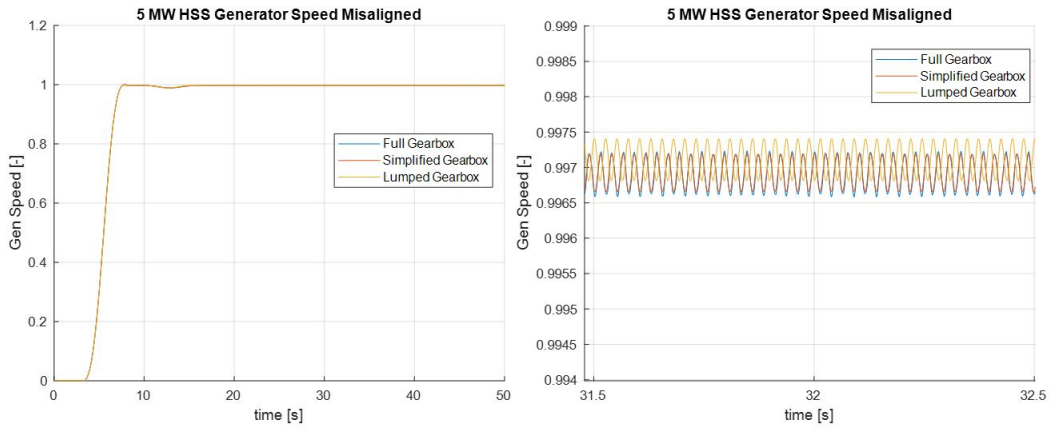


Figure 2.12: Generator Speed during misaligned steady state case

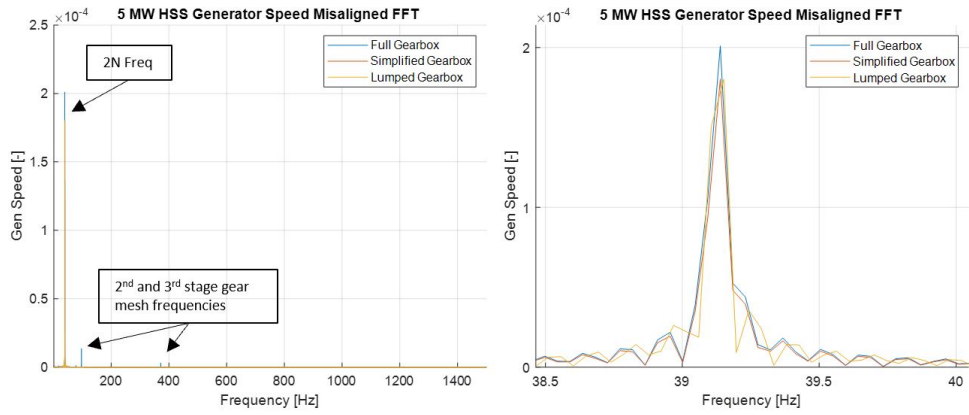


Figure 2.13: FFT of misaligned generator speed

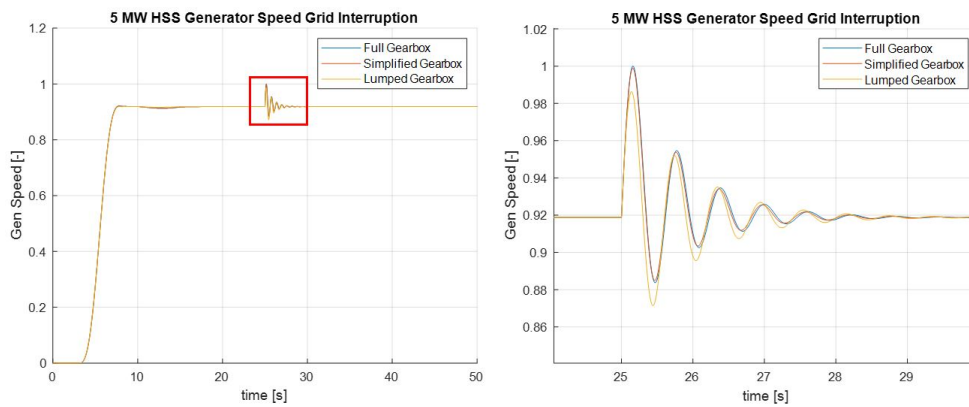


Figure 2.14: Generator speed for grid interruption event case

Table 2.2: Misaligned steady state generator speed frequencies captured by model configurations

Model Type	2N Frequency	Gear Mesh Frequencies
Full Gearbox	X	X
Simplified Gearbox	X	
Lumped Parameter	X	

2.6.3 Grid Interruption Event

After studying the turbine in different steady state conditions it is important to capture each model’s ability to replicate transient events. Each of the models produces a nearly identical response during the grid interruption event as shown in figure 2.14. The only differences originate from the error induced during the lumping process. The transient response of the 3 models is otherwise identical. This shows that each of these 3 models would be sufficient for use in electrical simulations focusing on electromechanical interaction in a turbine. Even in extreme transient events like a grid interruption the lumped drivetrain HSC model captures all the necessary components to provide a rotational velocity signal to electrical models. The simplicity of changing parameters as well as the extremely fast computation times can result in significant reduction in design times of electrical systems.

2.7 Bearing Load Study

2.7.1 Steady State Operation

To determine the changes in HSS bearing forces the response of the bearings under steady state operating conditions were investigated. The lumped parameter isolated HSC model was not used in this analysis as it does not contain any information on the bearings in the drivetrain. The plot of the axial bearing force of both models can be seen in figure 2.15. This plot shows that the simplified torsional gearbox model does sufficiently capture the axial force seen in the bearing, producing a force nearly identical to that seen in the full gearbox model. The simplified model however, does not capture the full dynamic loading seen in the bearing as a result of the gear meshing. These dynamic components are present in the full gearbox model due to the helix angle decomposition of the torque into the axial direction. This causes the torque to have a more significant impact on the axial loading on the bearing, which is not captured in the simplified model. The reductions in the

simplified model remove the meshing of the gears and thus a smaller dynamic loading is seen in the bearings.

The radial component of the DW tapered roller bearing (TRB) can be seen in figure 2.15. This plot shows the large differences in bearing load between the 2 fidelities. In the simplified model the lack of gear tooth slicing causes a portion of the radial force to be ignored seeing a reduction in static load of approximately 20%. As a result of the rigid bearing connections the load path is significantly changed making comparisons of bearing loads difficult. The UW cylindrical roller bearing (CRB) plot shown in figure 2.16 shows the large differences in dynamic loading not captured in the simplified model. Since the static load in the UW bearing was nearly identical a more detailed plot of the oscillations can also be seen in figure 2.16. The differences seen in this plot can be better interpreted through an FFT generated for the UW cylindrical roller bearing shown in figure 2.17. It can be seen that both models capture the 2N frequency generated from the HSC misalignment, however the other dominant frequencies in the response are all only seen in the high fidelity model. These frequencies all originate from the 2nd and 3rd stage gear meshing and it's subsequent harmonics. The 3rd stage meshing frequency has a larger amplitude due to its proximity to the HSS bearing. None of the meshing frequencies are captured in the simplified model and is the cause for the large differences in the amplitude of dynamic loading.

Table 2.3: Steady state UW bearing force frequencies captured by model configurations

Model Type	2N Frequency	Gear Mesh Frequencies
Full Gearbox	X	X
Simplified Gearbox	X	

2.7.2 Misaligned Steady State Operation

To determine the effect NTL has on HSS bearing forces it must be determined if each model can properly replicate the response of the drivetrain under severe NTL conditions. The plot of the force seen in the DW tapered roller bearing in steady state operation with induced misalignment can be seen in figure 2.18. The NTL used to achieve misalignment produces a static offset in the high fidelity model that is not captured in the simplified model. Removing DOFs from the gearbox caused a change in load path that prevents the loading in the bearing from being impacted correctly by the added NTL. As shown in figure 2.19, the radial force in the UW bearing is similar to the

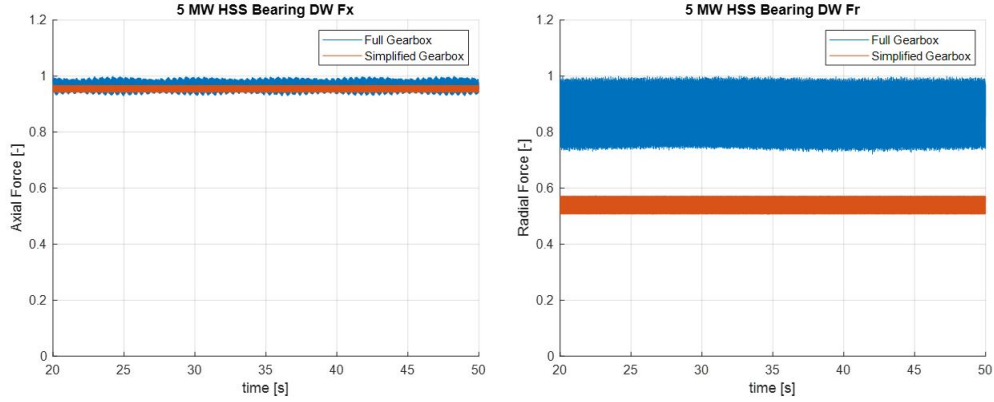


Figure 2.15: Time response of force in HSS DW tapered roller bearing in steady state operating conditions: axial component (left) and radial component (right)

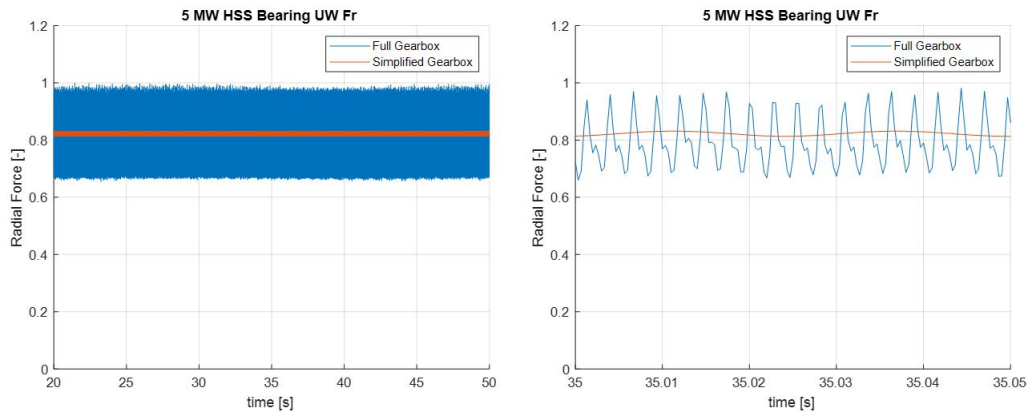


Figure 2.16: Time response of radial force in HSS UW cylindrical roller bearing in steady state operating conditions

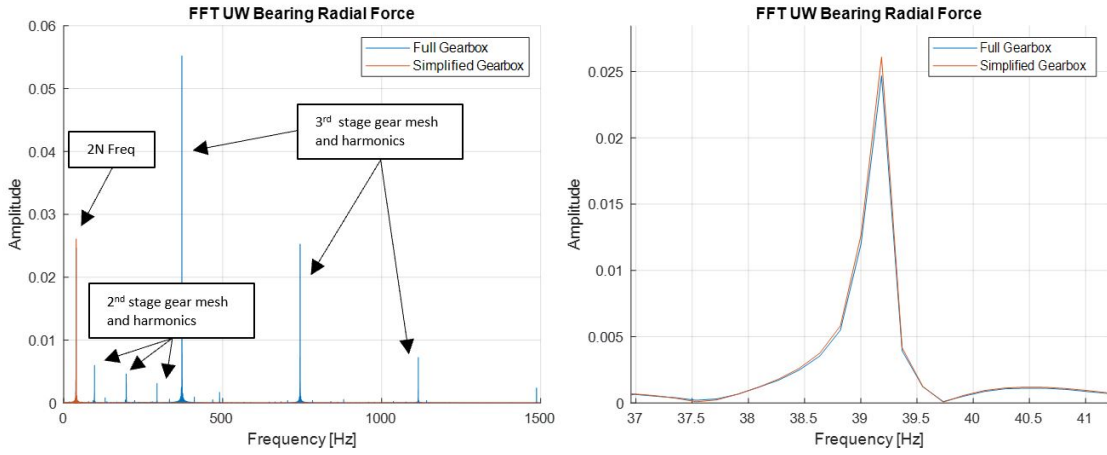


Figure 2.17: FFT of radial force in HSS UW cylindrical roller bearing in steady state operating conditions

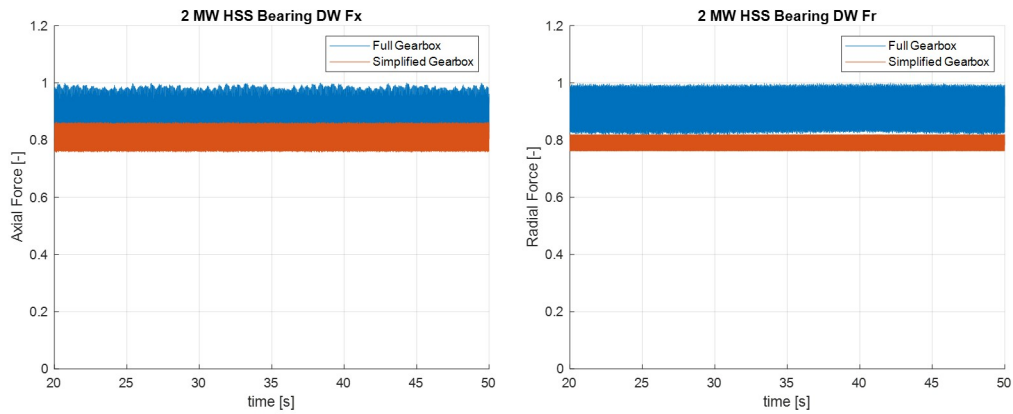


Figure 2.18: Time response of force in HSS DW tapered roller bearing in steady state misaligned operating conditions: axial component (left) and radial component (right)

steady-state generator speed response with minimal impact from the NTL.

2.7.3 Grid Interruption Event

A grid interruption event was simulated to determine the bearings response to a severe transient electrical event. The forces in the DW bearing are shown in figure 2.20. The plot of the axial component shows that the simplified model's lack of contact geometry prevents the model from capturing the full drop of loading seen in the bearing due to the grid interruption. The radial components do not have similar loadings at steady state so comparisons can not be made about the transience in the DW bearing. It can be seen in figure 2.21 that the simplified model replicates the transient responses during grid interruption well in the UW direction. This is to be expected as in each of the three test cases simulated, the UW bearing force is similar across the two models except for the dynamic loading.

2.8 Summary

Investigating each of the 3 model configurations for their ability to study electromechanical interaction yielded definitive results. From the electrical prospective each of the models used produces a nearly identical generator rotational velocity signal. The differences are small in magnitude and mostly originate from gear meshing frequencies not captured in the simplified and isolated component models. This analysis supports the accepted industry practice of running electrical simulations with isolated HSC models to capture the mechanical aspects of the turbine. Including only the HSC in electrical models can capture the 2N misalignment frequency and torsional slip in the HSC and the rest of the dynamics in the nacelle can be lumped. The computation times can be significantly reduced (about 28 times faster) and model changes implemented in a simpler manner than full system models. The simplified and lumped parameter models do not produce results sufficient for studying HSS bearing loading. The reduction of DOF in the drivetrain yields significant reduction in computation time but removes important aspects needed to capture the full behavior of the bearing. The isolated component model cannot be used as it does not contain any information on the bearings. In the following chapter the effects of the NTL on failure modes of the HSS bearings are studied. To that end, the high fidelity full gearbox model is utilized as it can capture of the effects of misalignment and gear contact.

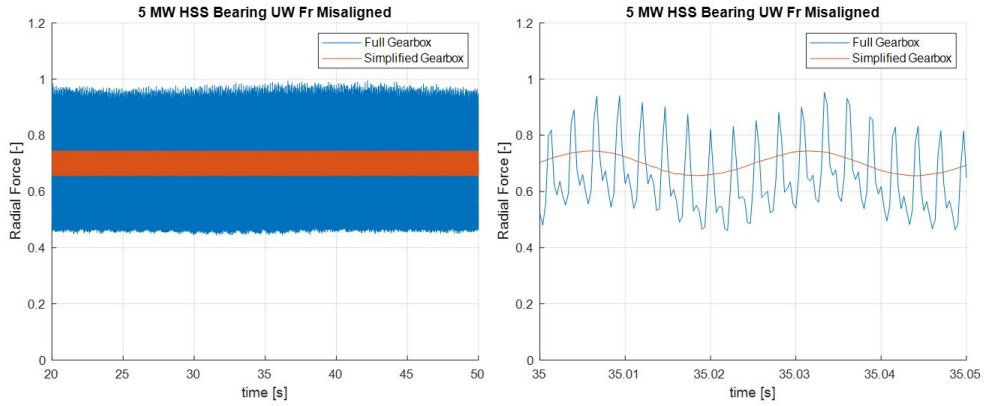


Figure 2.19: Time response of radial force in HSS UW cylindrical roller bearing in misaligned steady state operating conditions

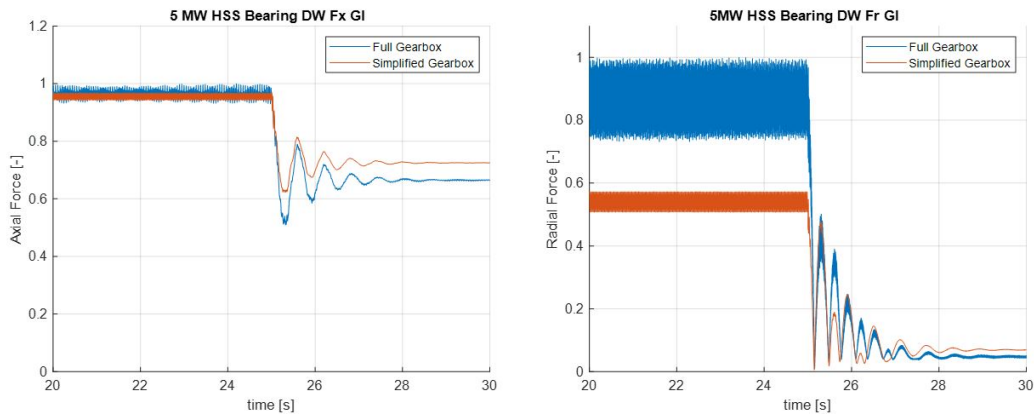


Figure 2.20: Time response of radial force in HSS DW tapered roller bearing during a grid interruption event

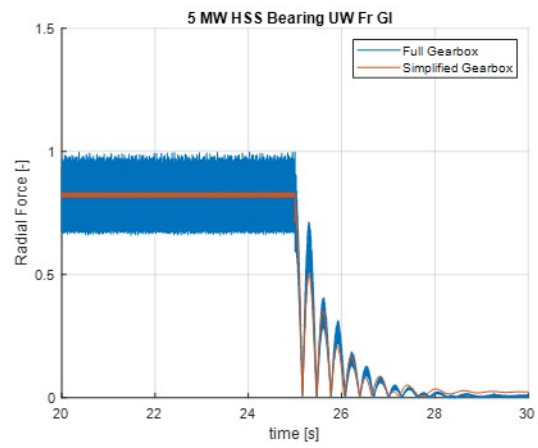


Figure 2.21: Time response of radial force in HSS UW cylindrical roller bearing during a grid interruption event

Table 2.4: Summary of model configurations

Model Name	Description	Total DOFs	Time Factor
High-Fidelity Full Gearbox	<ul style="list-style-type: none"> • Contains full contact geometry of gears • Captures individual tooth contact and meshing frequencies • Utilizes gear tooth slicing to account for misalignment and flexibility of the gear teeth • Support bushings and bearings used to provide flexibility of shaft and gear connections • Long computation times and file sizes • Difficult to build, some information required not readily available must be found experimentally • Hard to use, requires intimate knowledge of gearbox design to change test scenarios and run simulations 	325	41.24
Simplified Gearbox	<ul style="list-style-type: none"> • No individual gear tooth contact considered • Component inertias distributed throughout the drivetrain • Rigid connections that limit DOFs in the system • Significant improvement in computation time and file size • Requires less knowledge of the system to use, can still be difficult to operate without strong modeling background 	205	8.76
Isolated Component Lumped Parameter	<ul style="list-style-type: none"> • Lumps inertias of all components not of interest • Building an initial model can be time-consuming • Approximations are used at boundary conditions to replicate dynamics of the component inside the full system • Allows for one component to be put through a wide array of testing conditions very quickly • Often coupled to high fidelity electrical models to capture mechanical portion of turbine 	35	1.46

Chapter 3

Effects of Non-Torque Loading on High Speed Shaft Bearing Failure Modes

3.1 Drivetrain Model Selection

From the analysis in chapter 2 it was determined that a high fidelity full gearbox model was necessary to capture the full effects of NTL during grid interruption events on the HSS bearings. Two such models are utilized for the analysis in this chapter. The first is a 2 MW model previously developed by researchers at the EIC in coordination with the turbine's designers. This model was initially built for the purpose of mechanically simulating the response of an actual 2 MW wind turbine in extreme loading conditions and has since been adapted to meet the needs of this study. The second model utilized for this analysis is a 5 MW model initially developed as a benchmark for the industry by NREL. Researchers worked with various wind turbine OEMs to develop a full wind turbine model to be used as a baseline for study in the industry. The drivetrain model used in this analysis was isolated from the full wind turbine model developed and adapted to replicate the analysis performed on the 2 MW model. By using two different wind turbines, results can be checked for their agreement across designs and turbine size.

3.2 Grid Interruption Event Description

A wind turbine is a complex system that utilizes mechanical power from the wind to generate electrical power to the grid. The coupling of these 2 distinct aspects of a wind turbine is believed to be one of the leading causes of failure in the field. Some of the worst mechanical conditions in a wind turbine are produced as a result of electrical events. Sudden electrical events often lead to extreme mechanical reactions in the turbine. The best example of this can be seen in a grid interruption event. During normal operation, a wind turbine can often become disconnected from the grid, this results in a sudden loss of torque on the drivetrain from the generator. The sudden interruption from the grid causes a transient response in both the electrical components in the generator as well as the mechanical components in the nacelle.

When a fault occurs, the wind turbine often stops all power generation until the issue is corrected. During the interruption the voltage being supplied to the grid is interrupted and as a result the resistive torque from the generator is lost. After the back torque from the generator is lost the wind turbine speeds up while the aerodynamic torque driving rotation remains unchanged. As the turbine begins to accelerate the inertia of the turbine causes the torque to reverse several times before the system eventually reaches steady state again as seen in figure 3.1. This figure shows that while the torque continually changes direction and magnitude the speed remains fairly unchanged. As a result grid interruption events are studied extensively by wind turbine designers to ensure turbines can survive such severe events. It is essential that modeling techniques capture the wind turbines full behavior during grid interruption events so potential failures can be detected and then mitigated.

3.3 Test Profile Description

The goal of this analysis is to determine how NTL and subsequent misalignment in the drivetrain impacts HSS bearing failure during grid interruption events. To determine the impact these conditions have on potential failures, three test cases are constructed with varying amounts of NTL for two different wind turbine models. The NTL is modeled in the form of bending moments applied to the main shaft at the hub connection point to simulate the effects of the rotor blades and create misalignment in the drivetrain. The NTL is applied in its simplest form, statically and in only one direction, to simplify analyses. Actual NTL in a wind turbine is dynamic and influenced by

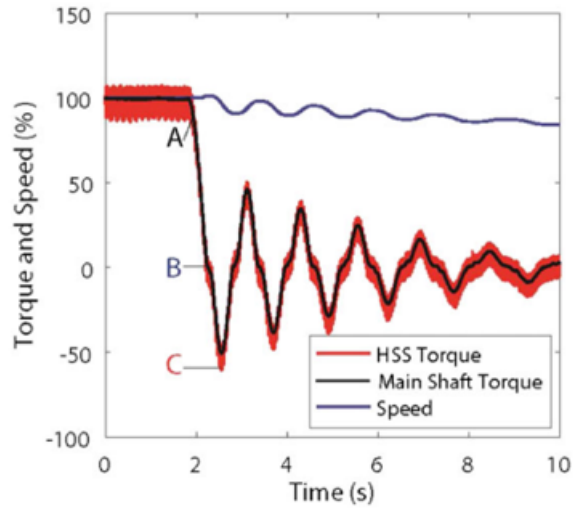


Figure 3.1: Torque and speed profile of high speed and main shaft during a grid interruption event [5]

the constant fluctuations in wind speed and direction. The NTL values in this study were chosen for the amount of misalignment they induce in the high speed shaft coupling at steady state operation. For both the 2MW and 5 MW models the largest NTL used or the 100% misalignment case was chosen to produce a misalignment close to the rated maximum of the high speed shaft coupling as seen in figure 3.3. The misalignment reported in these figures is measured from the generator end of the HSC to the gearbox end as shown in figure 3.2. The misalignment is only reported for the z direction as the other directions are negligible.

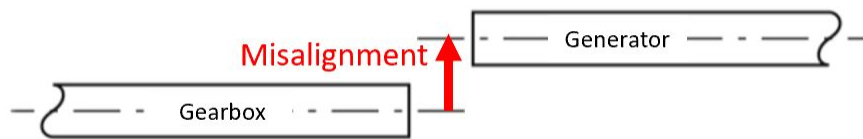


Figure 3.2: Diagram of HSC Misalignment

The 34% misalignment case for the 2MW model and the 23% misalignment case for the 5 MW model were chosen as they represent the turbines being started from the aligned position. Turbines in use today are designed for the HSC to be aligned with the weight of the rotor attached to the hub, this requires a NTL that is unique for each of the 2 models. In these isolated drivetrain models

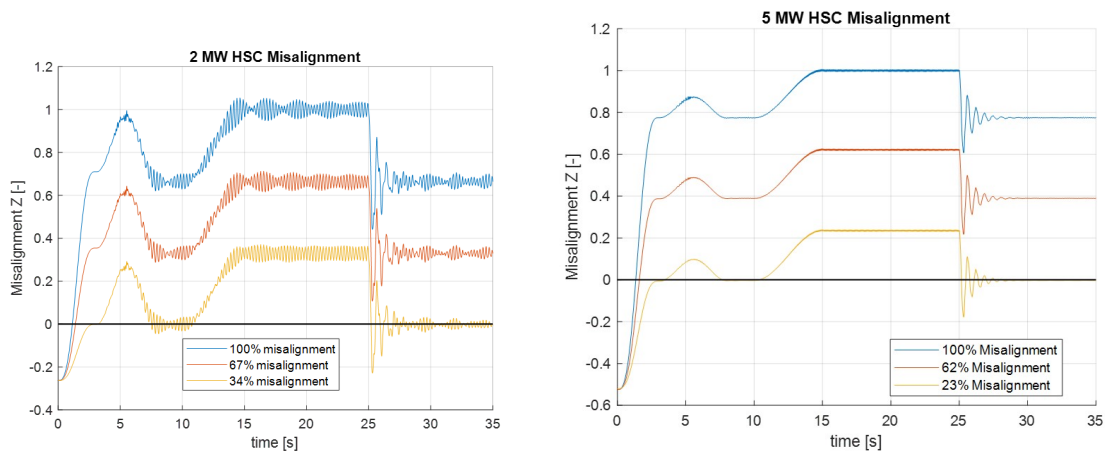


Figure 3.3: Time response of misalignment in the Z-direction of the high speed shaft coupling

the weight of the rotor is applied as a bending moment to bring the HSC into alignment. While this process brings the HSC into alignment before the wind turbine is in operation, the application of torque causes a phenomenon known as torque roll in the gearbox that induces misalignment in the high speed shaft coupling. Compliant torque arm mounts allow the gearbox housing to rotate and react the large torque values transmitted through the drivetrain, this in turn generates misalignment at the HSC as seen in figure 3.4. The 67% misalignment case for the 2 MW model and the 62% misalignment case for the 5 MW model were chosen to provide a linear relationship between the smallest and largest misalignments in each model.

It is important to note that the parameter values used in the 2 MW model are part of the wind turbine manufacturer's proprietary information and are not publicly available. As such, the bending moments applied are all divided by the maximum bending moment, as seen in figure 3.5. This same process is also used for the 5 MW model to keep the analysis consistent. Additionally, the transient responses are quantified as a normalized value in relation to the maximum steady state value of the signal. The responses in the figures to come in future sections can be viewed as a ratio of the force seen in the bearing to the maximum steady state force across each of the three test cases.

In the simulations used to model a grid interruption event with NTL and misalignment, the procedure is as follows. First the bending moment is applied to induce misalignment in the system. Next the the turbine must be brought up to speed, as a grid interruption event can not be simulated

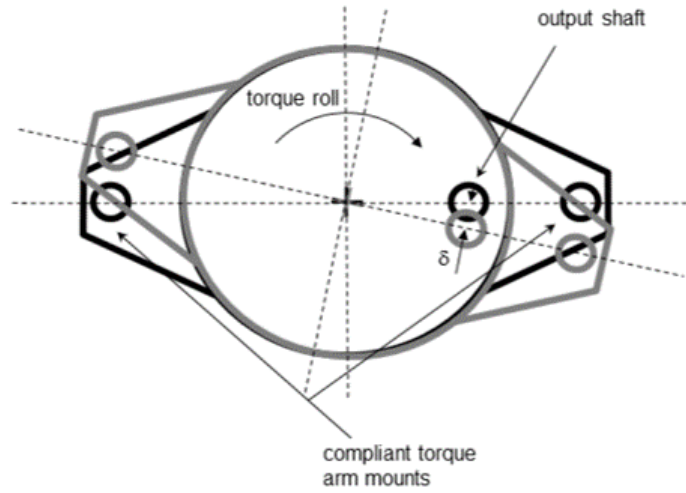


Figure 3.4: Displacement of gearbox under load induces HSC misalignment [18]

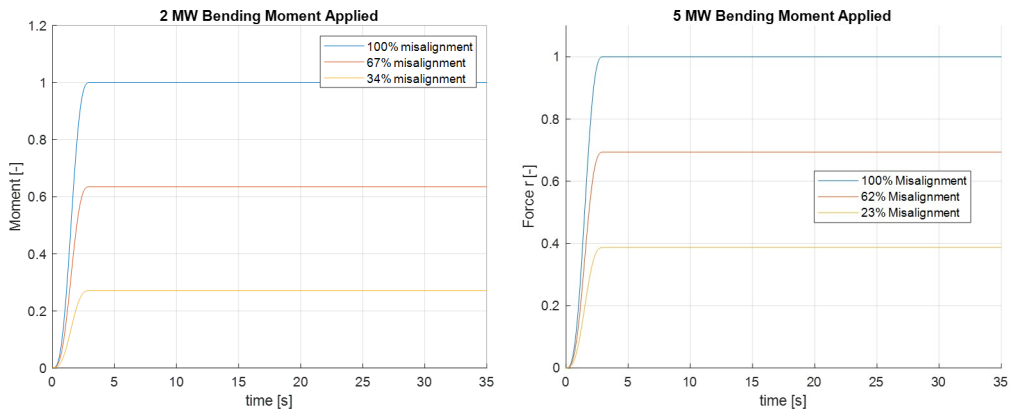


Figure 3.5: Bending moments used to model NTL in 2 MW (left) and 5 MW (right) test profiles

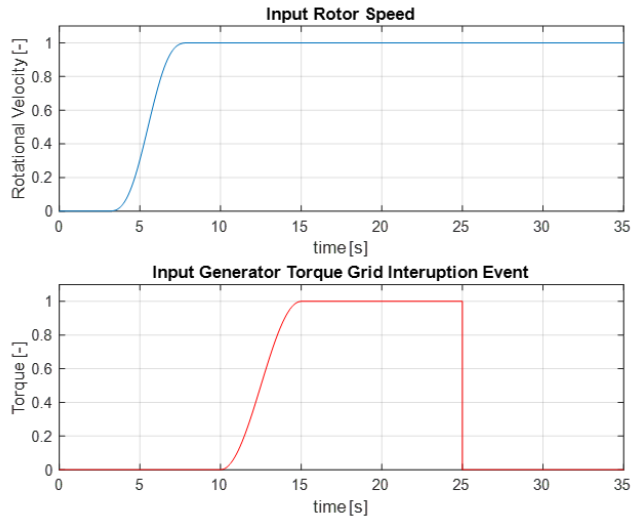


Figure 3.6: Test profiles used to model grid interruption events, generator back torque (top) and rotor speed (bottom)

unless the turbine is already operating at steady state. The drivetrain is brought up to speed with a PI speed controller and the velocity profile used as a reference input is shown in figure 3.6. After the model is up to speed the back torque can then be applied, as it resists the rotation of the turbine. Once the model reaches steady state again the grid interruption event can be implemented. This is done at the 25 second portion of the test profile utilizing the generator torque signal, as seen in figure 3.6. Reducing the generator torque to zero represents loss of grid connection. Such a profile can be used to study the mechanical responses in a wind turbine drivetrain.

3.4 Gear Mesh and Bearing Force Reactions

Fundamental to the analysis in this report is the understanding that the torque transmitted through the drivetrain is a driving component of the loading in the HSS bearings. Each of the gears used in the wind turbines in this analysis are helical gears. Helical gears utilize angled gear teeth to minimize noise and vibration while transferring larger torques than other types of gears. To understand the transmission forces between helical gears a few parameters must be known. The first is the pressure angle (ϕ) which can be seen in figure 3.7, this angle is the relationship between the line of contact of the gear teeth and the pitch circle. This angle is created by the contact between

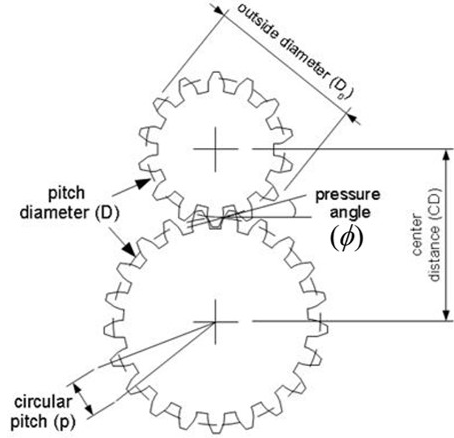


Figure 3.7: Pressure angle diagram [8]

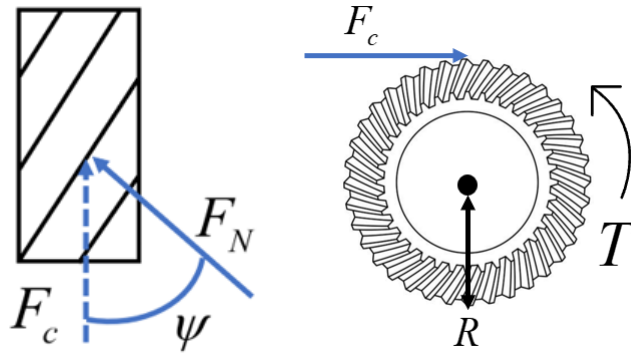


Figure 3.8: Helix angle diagram (left) Helical gear free body diagram (right)

two gear teeth and decomposes the total transmission force into a component normal to the gear teeth and a radial component normal to the pitch circle. For a helical gear the normal force (F_N) is decomposed again as the gear teeth are not parallel to the axis of rotation. The helix angles of the gears (ψ), shown in figure 3.8 decomposes the force normal to the gear teeth into a circumferential component (F_c) that drives rotation and an axial component (F_x). The FBD for a helical gear fixed to a shaft can be seen in figure 3.8 and yields equation 3.1 when rotating at a constant velocity. Using these decompositions to work backwards from equation 3.1 the transmission forces in terms of torque can be written as shown in equations 3.2 and 3.3, where F_r is the radial force and F_x is the axial force generated by the gear meshing.

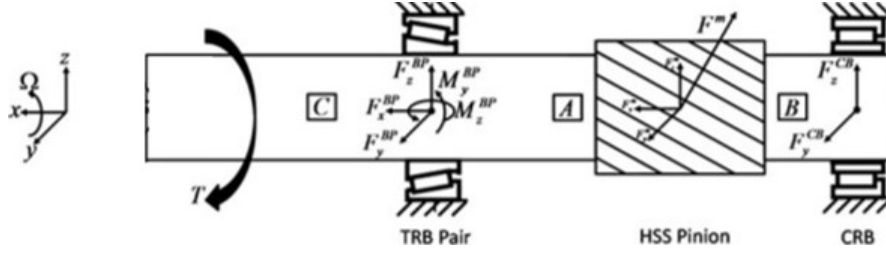


Figure 3.9: Free body diagram of high speed shaft [5]

$$\Sigma M_x : T = F_c R \quad (3.1)$$

The free body diagram for the HSS in a wind turbine can be seen in figure 3.9. From the equations for the gear transmission forces, it is clear that they are directly proportional to the torque in the drivetrain. As such, torque release during an event such as the grid interruption will significantly impact the loads on the bearings. A transient event like a grid interruption that removes all torque from the drivetrain should have a significant impact on the load in the bearings.

$$F_x = \frac{T}{R \tan \psi} \quad (3.2)$$

$$F_r = \frac{T \tan \phi}{R \cos \psi} \quad (3.3)$$

3.5 Bearing Failure Modes

To determine the effect NTL has on bearing failure, the loading in the bearings will be investigated for two potential failure modes, the first of which is impact loading on the bearing. During grid interruption events the torque in the drivetrain is reversed rapidly and can lead to large amplitude forces inside the bearing being reversed very quickly. Such dynamic shifts in the contact zone of the bearing can result in significant damage or even failure. In this model, the contact geometry for the bearing is not used; however, by measuring the force the bearing provides in the

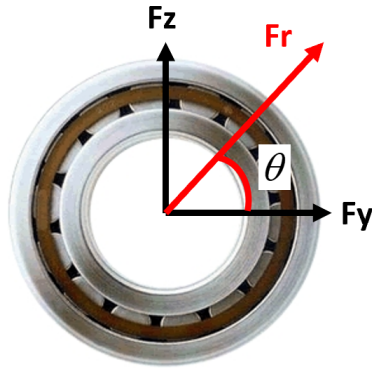


Figure 3.10: Bearing radial force decomposition

y and z directions the radial force and contact angle can be approximated. Figure 3.10 shows a cylindrical roller bearing with the radial force and its corresponding contact angle. Any significant shift in the angle of contact of the bearing in a short period of time would be cause for concern. Impacts on the bearing can cause plastic deformation or fractures that reduce the lifespan of the bearing. As a result, the bearing force contact angles were investigated for changes during grid interruption events with varied NTL applied.

The second potential failure mode of the bearing investigated is skidding. High speed rolling element bearings require sufficient loading in order to prevent sliding between the rolling elements and the raceway (i.e. skidding). Skidding occurs when the tractive force between the raceway and the rolling element is insufficient to overcome the cage drag and churning losses [18]. In simple terms the forces in the bearing need to be large enough to engage the bearing during operation. Some bearing applications utilize preloading in the bearings to ensure that bearing forces are never brought out of engagement. However, loading in wind turbines is much more dynamic than traditional applications and designs often seek to reduce bearing costs by limiting the loading seen in the bearing. Skidding becomes increasingly troublesome when the bearing is operating at high speeds as the effects are magnified by a high number of revolutions during the phenomenon. In wind turbines, a grid interruption event poses one of the worst case scenarios, where a bearing is operating at a high speed under large torque. The loss of torque during operation can cause bearings to rotate at high speeds without enough force to properly engage the bearing and prevent skidding.

3.6 Bearing Loads Under Static Non-Torque Loading

The following results were generated by simulating a torque release during steady state operation of a wind turbine with various amounts of NTL applied statically. The effects will then be noted on each HSS bearing, starting with the DW tapered roller bearing (TRB). The plots of the both model's TRB axial components are shown in figure 3.11. In the 2 MW model the bearing sees a reduction in load as a result of the NTL applied. This is a primary concern when determining if skidding is to occur. While the bearing force remains above 20% of the steady state maximum in both cases, the misalignment values chosen were conservative and with the NTL only applied in one direction. This presents a scenario in which NTL can be applied at a large enough value to create a loading much closer to zero in the bearing. In the plot of the 5 MW model's axial component, the loading in the bearing increases with the application of NTL. In this case the NTL creates a force in the same direction as the preloading. The difference in preloading direction between the 2 models can be attributed to unique design considerations between the 2 and 5 MW turbines. Both of these models show agreement that the presence of NTL during a grid interruption event could be a potential cause of conditions that give rise to skidding in the bearings.

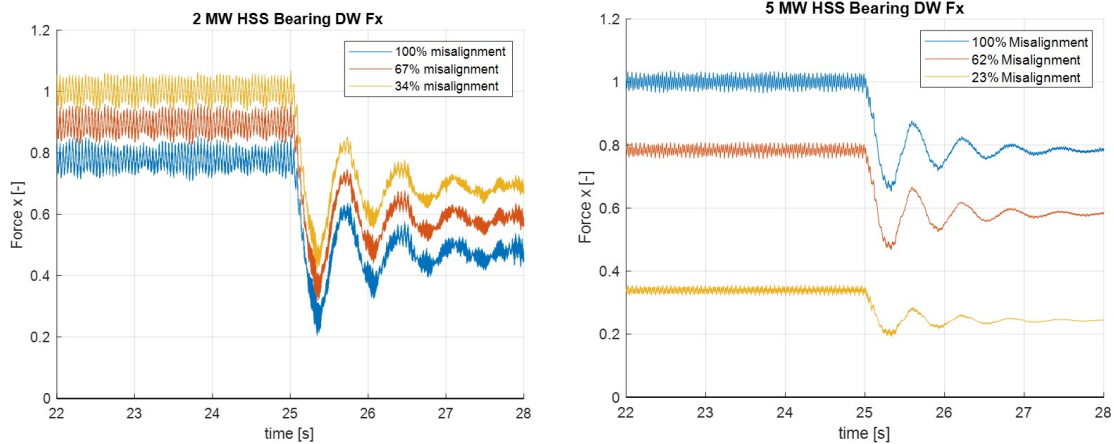


Figure 3.11: Time response of 2 MW (left) and 5 MW (right) tapered roller bearing axial force during a grid interruption event

Similar to the loading in the axial direction the radial component of the tapered roller bearing force in both models is shown to shift statically with the application of NTL, which can be seen in figure 3.12. The value used to report the radial force is a magnitude which does not

allow for negative values, the direction is accounted for using the contact angles instead. This is misleading as all 3 cases in both models appear to have nearly identical loading at steady state. In reality the 67% and 100% misalignment cases are both loaded in the opposite direction of the 34% case, but similar in magnitude. The impact of NTL can be better seen after the interruption, where each of the cases with added NTL do not approach 0 load and instead are shifted away from 0. By increasing the minimum radial load seen in the bearing during the grid interruption event, NTL has the potential to alleviate concerns of skidding in the bearing. This is a potential improvement in bearing behavior as one of the main concerns during grid interruption events is the bearing load becoming near 0 while the speed of the HSS is still high.

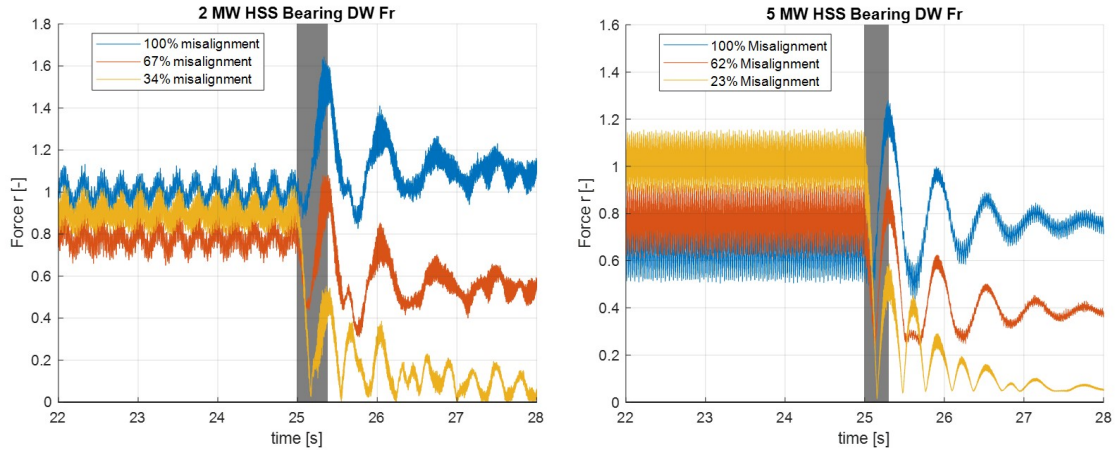


Figure 3.12: Time response of 2 MW (left) and 5 MW (right) tapered roller bearing radial force during a grid interruption event

In both models the UW cylindrical roller bearing responds in much the same way as the DW bearing as can be seen in figure 3.13. The main impact of the NTL again is a static shift in the loading in the turbine causing the bearing to avoid potential cases of skidding. Both models show that adding NTL causes the loading during the grid interruption event to be non-zero during the transients. The 34% and the 23% each see loading near 0 during the interruption, however the cases with added NTL do not. This again shows adding NTL can alleviate skidding concerns in the UW CRB as well. For both bearings the three cases experience significant transience when the grid is interrupted with the force changing magnitude very quickly. The first torque reversal seen from the grid interruption occurs in approximately 0.3 seconds causing severe oscillations in the bearing force. To better understand the loading in the bearing during the transient event a more

isolated plot during the interruption must be used. Polar plots were used to show the force and corresponding contact angle at each time instance during the grid interruption event.

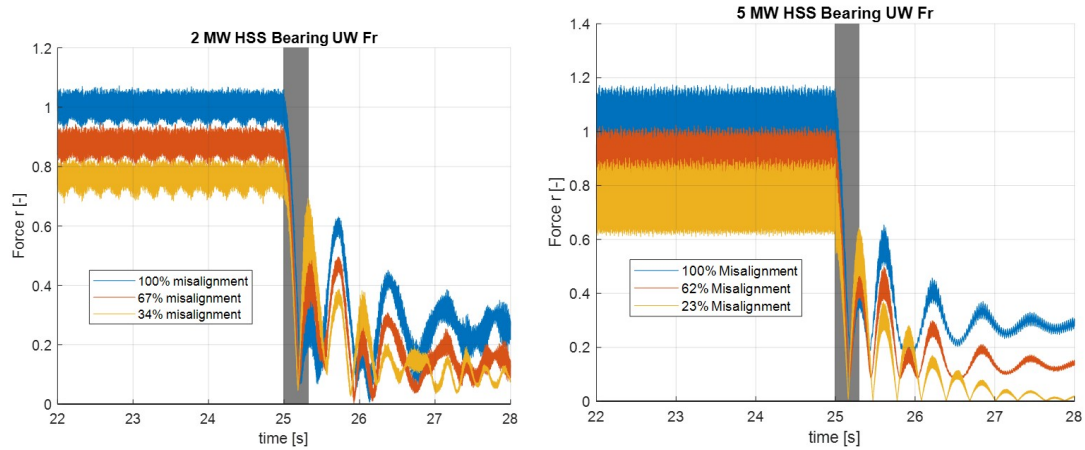


Figure 3.13: Time response of the 2 MW (left) and 5 MW (right) cylindrical roller bearing radial force during a grid interruption event

Figures 3.14 and 3.15 show the contact angles and radial force of the two bearings in both models during the first torque reversal in a grid interruption event. The portion of the response of each bearing used in the generation of these polar plots is highlighted in each of the previous bearing force plots. Only the first reversal is used for these plots as the behavior in the subsequent torque reversals is nearly identical with a reduced amplitude as the oscillations are damped. The loading shown in the plot all occurs in about 0.3 seconds, causing a significant impact load on the bearing in each of the cases. The NTL applied can be seen to lower the change in contact angle significantly in the DW TRB, as seen in table 3.1. The added loading moves the oscillations away from 0, causing the reversals to be inside a smaller area of the bearing. This means the impact loading in the bearing can be reduced by applying NTL. Both tapered roller bearings also show that applying NTL can shift the reversals away from 0 removing concerns of skidding. In the more aligned cases the reversals pass through a 0 load zone while the speed of the shaft is still exceptionally high, this is highly likely to cause skidding in the bearings. Applying NTL of the correct magnitude reduces the change in angle and causes the bearing to not pass through the 0 loading zone in its transience. The results from this analysis show that NTL can be beneficial to both of the main failure modes of the HSS DW TRB.

The results for the HSS UW CRB were not as conclusive as the DW TRB. In the 2 MW

model shown in figure 3.14 the addition of NTL had minimal impact on the angle reversed as well as the minimal radial load seen in the bearing. The minimal radial load in the UW bearing was seen to increase slightly with application of NTL possibly lessening the effects of skidding in the bearing, but this came with the trade-off of increasing the change in contact angle during the grid interruption. The 5 MW UW CRB, shown in figure 3.15, experiences a reduction in change in contact angle as well as an increase in minimal load experienced during the grid interruption. These observations show that in the 5 MW model NTL has the ability to alleviate both potential failure modes and improve the life of both HSS bearings. While not conclusive for the 2 MW model added NTL also shows the potential to at the very least improve the lifespan of the DW TRB while minimally impacting the UW bearing.

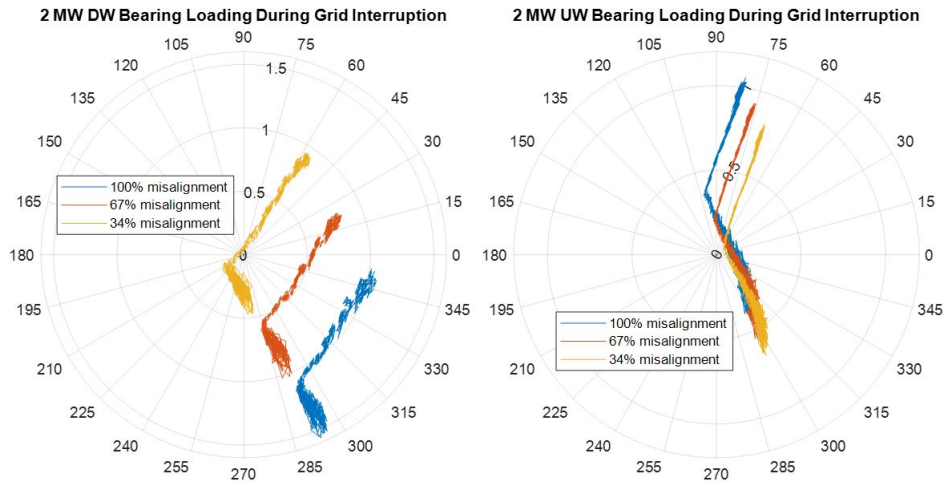


Figure 3.14: 2 MW bearing loading zones during a grid interruption event

Table 3.1: Grid interruption transience of 2 MW and 5 MW models with static NTL

Model	Misalignment	DW Reversal Amount	DW Minimum Radial Load	UW Reversal Amount	UW Minimum Radial Load
2 MW	100% Misalignment	55°	.873	146°	.067
	67% Misalignment	93°	.439	141°	.064
	34% Misalignment	154°	.026	135°	.045
5 MW	100% Misalignment	106°	.448	120°	.183
	62% Misalignment	130°	.237	134°	.089
	23% Misalignment	150°	.015	143°	.007

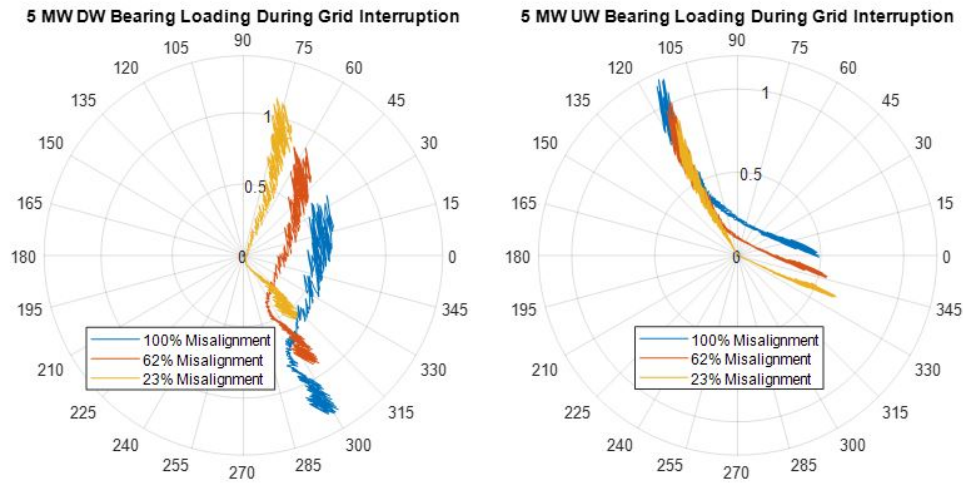


Figure 3.15: 5 MW bearing loading zones during a grid interruption event

3.7 Summary

The results from both models are in good agreement with respect to bearing forces generated during transient events. Both models showed that the NTL does have an impact on the forces seen in the bearings. The impact on the bearings was in most cases just a DC offset in the force signal, however effects of these shifts are significant. Current component lifespan estimation techniques neglect NTL when considering the lifespan of the bearings as torque is thought to dominate the loading of the bearing. While torque does drive most of the load in the bearing it was seen in both models that changes in NTL could aid in creating conditions that lead to premature failure in the HSS bearings. In this study NTL was found to have a potential benefit on bearing health. For both the failure modes considered adding NTL was found to reduce the change in contact angle of both bearings as well as, increase the minimal radial load experienced by each bearing. By increasing the minimal radial load the bearing experiences during a grid interruption, NTL can be used to prevent cases of skidding in the bearings. Similarly, adding NTL caused the change in contact angle in the bearing to decrease significantly, creating less impact loads during a grid interruption. Reducing the change in contact angle can lead to less micro-fractures and deformation and extend the life of the bearings as well. This analysis shows the potential benefits of adding NTL to the drivetrain, which leads to the question of how NTL can be implemented to achieve these potential benefits? This will be discussed at length in the following chapter.

Chapter 4

Effects of Generator Offset on High Speed Shaft Bearing Failure Modes

4.1 Application of NTL to Drivetrain

In the previous chapter it was determined that NTL has the capability of extending the life of the HSS bearings by shifting the loading zone away from potential skidding situations and lessening the impact loading seen during a grid interruption event. If turbine manufacturers are to utilize NTL to remove skidding and impact loading concerns on the HSS bearings the question remains of how to implement NTL into the turbine? In the previous chapter NTL was chosen for its ability to produce misalignment in the HSC. One method to achieve misalignment in the HSC would be to shim the generator and induce a preloading in the HSC that generates a static NTL on the drivetrain.

To ensure this method can produce the desired results seen in the previous chapter, the 2 MW 67% misalignment case was replicated by shimming the generator to induce the misalignment reached during the application of the bending moment as seen in figure 4.1. This shows that offsetting the generator can reproduce the steady state misalignment in the HSC as seen in the previous chapter. Next the generator offset must be checked for its ability to replicate the HSS bearing forces seen during the previous study. The HSS tapered roller bearing loads can be seen in the previous 67% misalignment case as well as the new "shimmed" case in figure 4.2. This plot shows

there are minor differences between the moment being applied at the hub and the misalignment being applied at the generator. The same can be said for the radial loading in the DW TRB and UW CRB shown in figures 4.2 and 4.3 respectively.

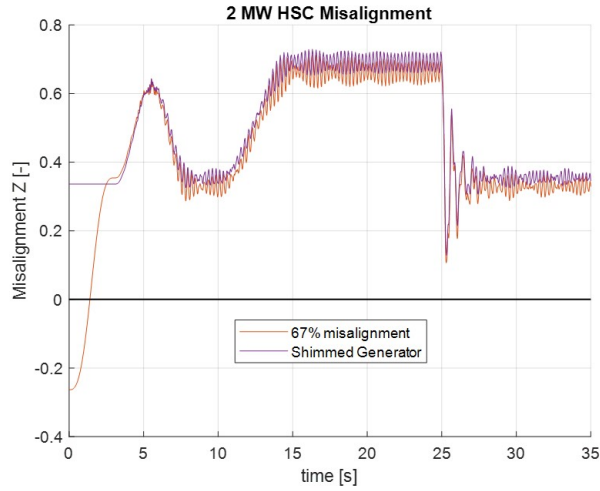


Figure 4.1: Comparison of offset generator vs applied NTL on HSC Misalignment

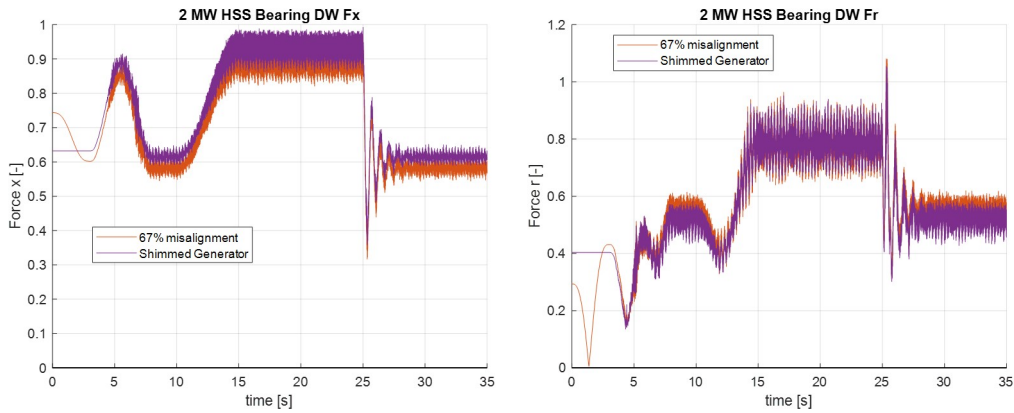


Figure 4.2: Comparison of offset generator vs applied NTL on tapered roller bearing axial force during a grid interruption event

The most important ability of the shimmed model is its ability to replicate the transience seen during the grid interruption event. This can be seen in the contact angle vs radial load plots shown in figure 4.4. These plots show that the dynamic behavior of the wind turbine during a grid interruption event is nearly identical. The changes in contact angle and corresponding radial force

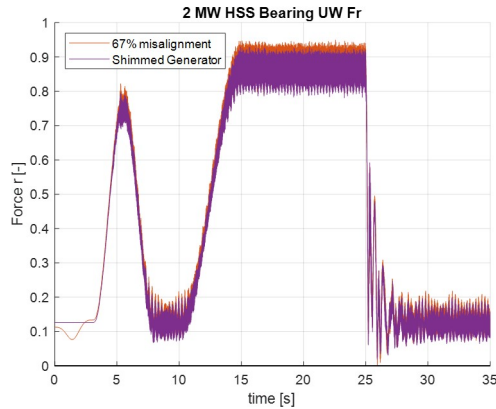


Figure 4.3: Comparison of offset generator vs applied NTL on cylindrical roller bearing radial force during a grid interruption event

are in very good agreement thereby demonstrating that the shimmed generator model can be used to study the effect of NTL in field conditions.

4.2 High Speed Shaft Coupling Alignment Considerations

The previous chapters analysis showed that the more NTL added to the drivetrain, the less impact loading and skidding were experienced during a grid interruption. These two benefits come at a cost of additional loading on the components as a result of misalignment in the drivetrain. While the HSC is designed to allow misalignment between the gearbox and the generator, it is not desired. Misalignment in the HSC is known to produce high frequency vibrations and increase axial and radial loading on components, increasing fatigue damage [16]. This added loading can be damaging to components and lead to premature failure. For this reason turbine designers seek to align the components as best they can during installation to minimize the misalignment present during operation.

Wind turbines in operation today have HSCs that were aligned in the static sense, that is, while the turbines were not operating. The weight of the rotor is a large source of NTL on the drivetrain and as a result the order in which components are installed is very important. When installing the HSC it is common practice to install the HSC and the rotor and then align the system as the added rotor weight can bring the system out of alignment [7]. As shown in figure 4.5, the misalignment due to the added rotor weight is offset by using shims to increase the height of the

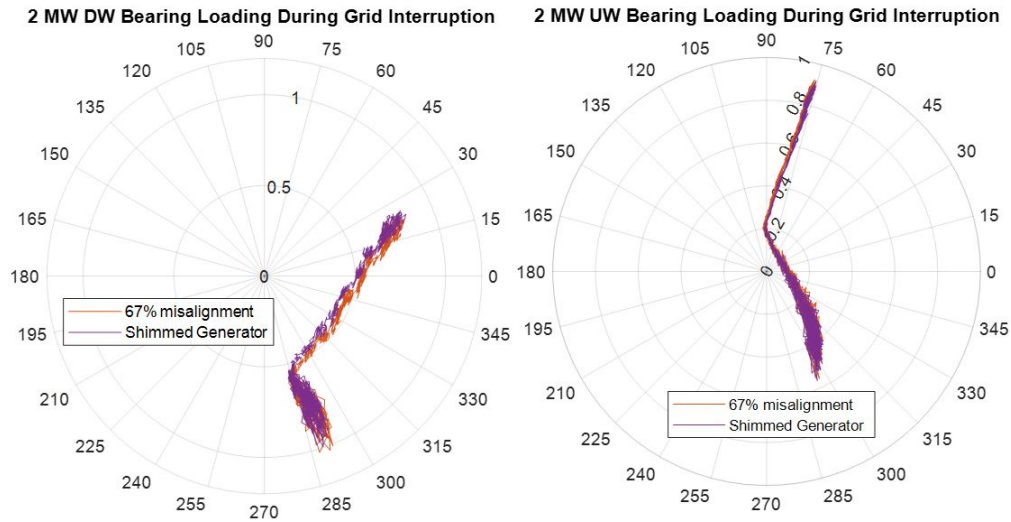


Figure 4.4: Comparison of offset generator vs applied NTL on bearing loading zones during a grid interruption event

generator and align the HSC. While this method of aligning couplings has been common place for years, the high failure rates of the HSS bearings and their proximity to the HSC, point to the need to reevaluate if this is in fact the best practice.

The goal of the current static alignment procedure is to reduce unnecessary loading on components. However, it has been shown previously that when the turbine is running, applying torque induces a misalignment in the drivetrain. The misalignment in the turbine during the ramp up to steady state operation for a conventionally aligned drivetrain can be seen in figure 4.6. The

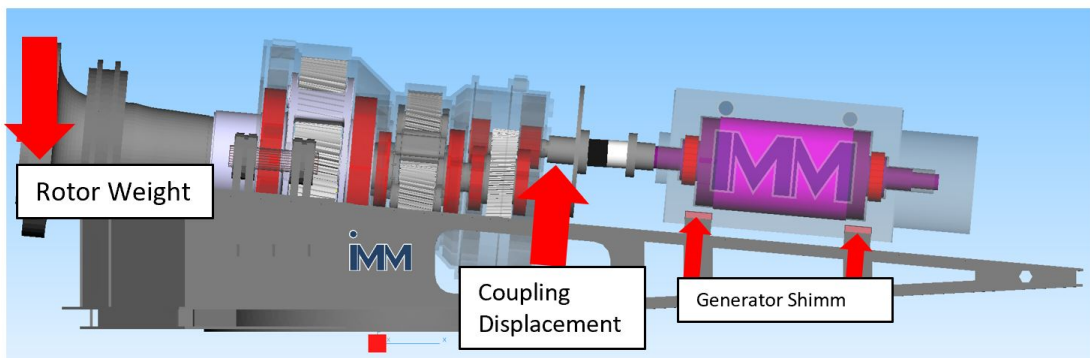


Figure 4.5: Rotor Weight Induced Misalignment

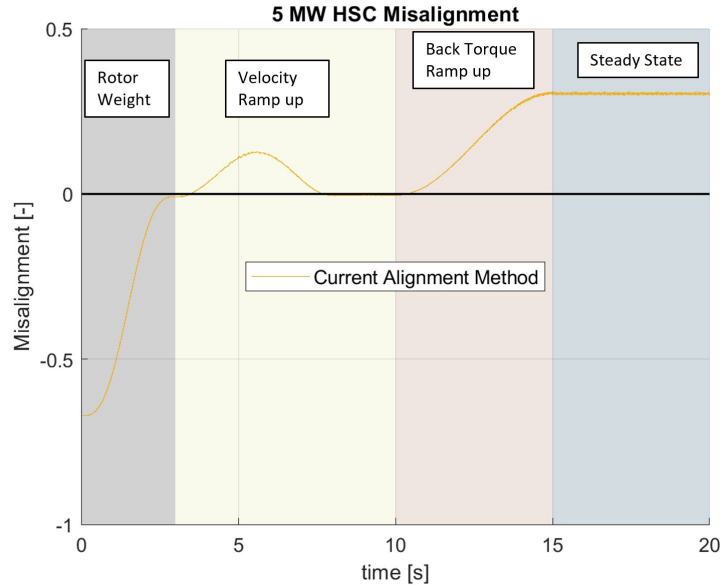


Figure 4.6: Operational misalignment of a statically aligned HSC

turbines used for this study already include the alignment with the rotor weight applied, so the generator offset is already specified. The rotor weight is applied in the first portion of the test profile to visualize the effect of the alignment on the stationary turbine (see Fig. 4.6). It is apparent from the figure that a significant amount of misalignment is still present in the drivetrain during steady state operation.

The current procedure ignores the torque roll induced misalignment and causes the turbine to become misaligned during steady state operation. This misalignment could be leading to excessive loading on components reducing their lifespans. Additionally it was seen in the previous chapter that in the statically aligned cases the loss of torque in the drivetrain coupled with the lack of NTL lead to more significant force reversals in the HSS bearings, passing through the 0 load zone creating cases of skidding and potentially reducing the life of bearings.

Wind turbines typically spend 95% of their lifespan in operation [19]. As a result, it is important that the alignment procedure accounts for misalignments during normal operation. Instead of aligning the HSC for when it is not in operation, the alignment should be performed dynamically, taking into account the torque roll induced misalignment and aligning the coupling for steady state operation. Aligning the system with the torque applied would be a manner of applying static NTL to the system as it was studied in the previous chapter. As shown previously, applying NTL can

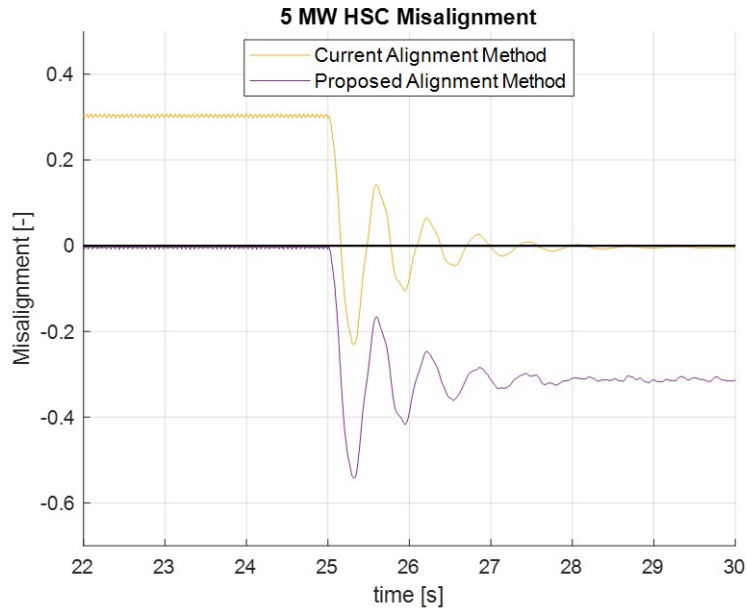


Figure 4.7: HSC Misalignment during a grid interruption event of a dynamically and statically aligned HSC

prevent zero crossing and thereby skidding in the loading zone of the bearing particularly during grid interruption events.

A turbine aligned conventionally sees the loss of torque during a grid interruption event and returns to an aligned coupling with no NTL and can experience skidding. However, if the coupling was aligned dynamically, with torque applied, the loss of torque during the grid interruption event would bring the coupling out of alignment causing the load in the bearing to stay above zero potentially removing concerns of skidding shown in figure 4.7. Each of these potential benefits motivates the need for study if this new alignment method can improve the failure rates of HSS bearings.

4.3 Proposed Alignment Procedure

A new procedure for aligning the HSC would allow for many of the benefits of adding NTL to the drivetrain to be utilized without adding additional loading to components. This new procedure would be very similar to current methods of aligning the HSC in use today with a few added steps. The dynamic alignment procedure would be as follows:

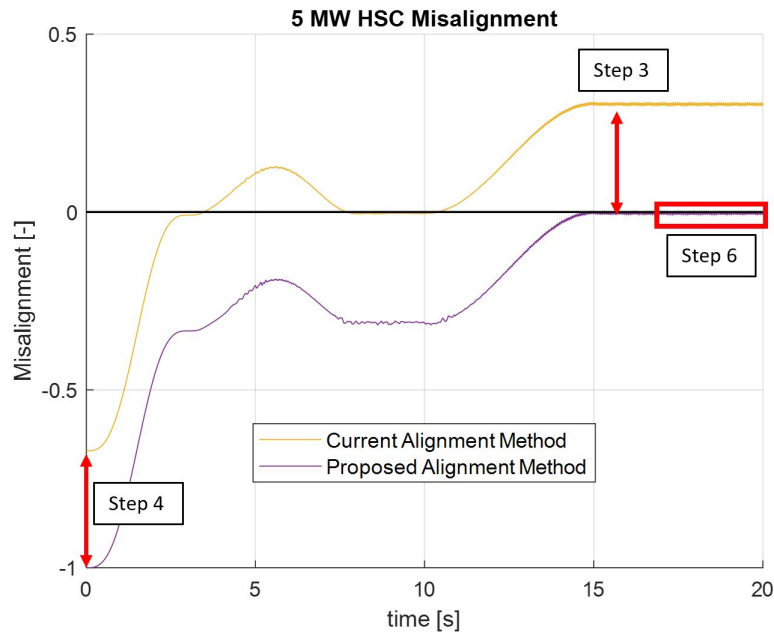


Figure 4.8: Procedure for dynamically aligning HSC

1. Install the drivetrain to the tower in the conventional manner
2. After installation is finished allow the turbine to ramp up to full rated power
3. Measure misalignment of high speed shaft coupling when under load
4. Add offset to the generator equal to the displacement seen during operation
5. Allow the turbine to return to full rated power
6. Measure misalignment of high speed shaft coupling at rated power and ensure alignment

This process can be visualized in figure 4.8, where it can be seen that alignment of the HSC under load is achieved to a reasonable level of accuracy. Rather than measuring the displacement of the HSC, wind turbine designers could utilize knowledge of the turbine to determine the amount of misalignment that would be induced to a limited degree of accuracy and recommend an amount of misalignment in the HSC during installation. With this new method of aligning the HSC, it now must be determined if dynamic alignment will indeed improve the performance of the HSS bearings.

4.4 Offset Generator Bearing Response to Grid Interruption Events

To determine the effectiveness of this new alignment method of offsetting the generator to account for torque induced misalignment, two cases were used. Each case was generated for both the 2 MW and 5 MW models to check for agreement across turbine designs. The first case was the conventionally aligned case as used in the previous chapter. This case was referred to as the 34% case in the 2 MW model and the 23% case in the 5 MW model. Each of these cases represent the turbine starting operation with the HSC aligned and ramping up to rated power. Once at rated power the grid connection was interrupted removing the back torque from the system as shown previously. The torque induced misalignments from these two cases were then used to offset the generator in both the models to obtain the new alignment. Figure 4.9 shows a comparison of the misalignment in the HSC obtained from current and proposed alignment methods when simulating a grid interruption event. By comparing the bearing loads in each of these cases it can be determined if the benefits shown in chapter 3 can be replicated while removing operational misalignment from the system.

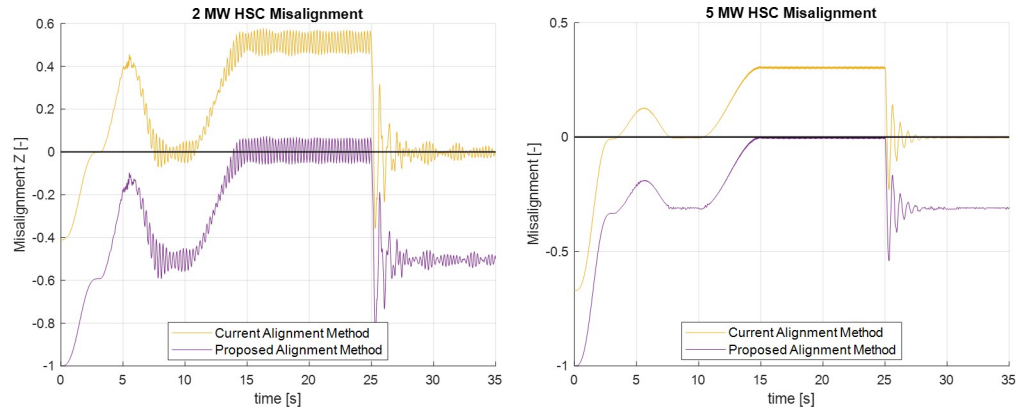


Figure 4.9: Dynamic wind profile grid interruption event set values

The axial loading in the DW tapered roller bearings can be seen in figure 4.10. The addition of NTL through the implementation of generator offset caused larger loading in both models axial components. The same can be said for the radial force in the DW TRB as seen in figure 4.11. In all cases except the 2 MW axial force, the load increased by approximately 30% of the steady state loading in the bearing. This is a significant increase in the loading, which should not be ignored.

Depending on the design of the turbine this increase in loading could be detrimental to the life of the bearing. However most turbine bearings are designed for extreme wind cases and significantly higher loads than the ones seen in this analysis. The increase in bearing load for the proposed dynamically aligned HSC is not the expected result as bringing the HSC into alignment was thought to reduce the overall load in the bearings. This shift in loading could be explained by the reduction of misalignment causing the loading to become more evenly distributed across the 2 HSS bearings. Nevertheless, this increase in loading should be investigated further for the effects it might cause on the bearing.

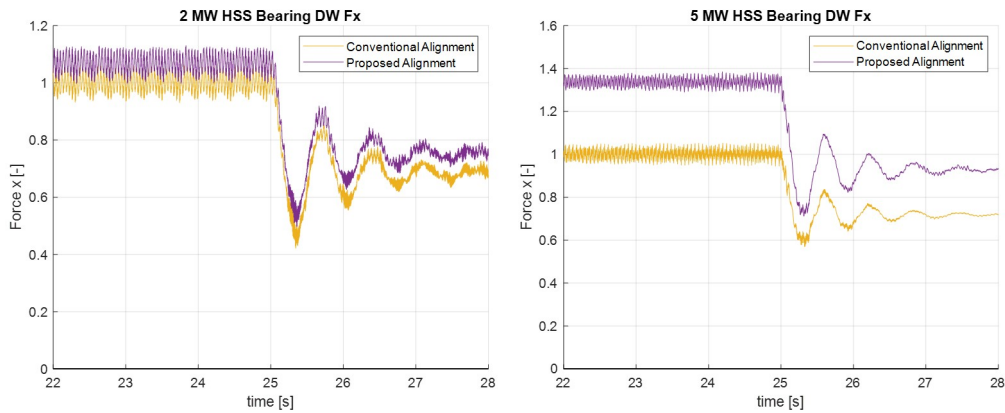


Figure 4.10: Axial loading in 2 MW (left) and 5 MW (right) DW Tapered Roller Bearing during grid interruption event of 2 alignment methods

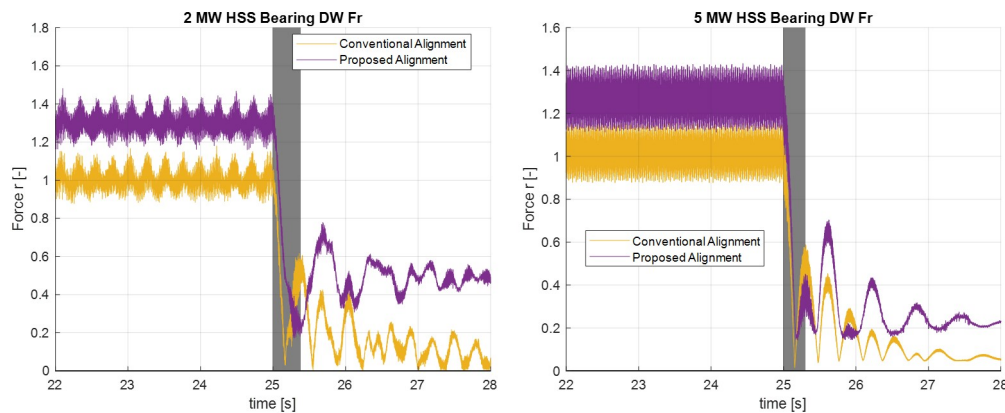


Figure 4.11: Radial loading in 2 MW (left) and 5 MW (right) DW Tapered Roller Bearing during grid interruption event of 2 alignment methods

The force in the UW bearing for both the 2 MW and 5 MW models is reduced in the dynamically aligned cases as can be seen in figure 4.12. Both models agree that the removal of misalignment in the HSC during steady state operation reduces the loading in the UW bearing. Dynamically aligning the HSC shows a reduction of about 10% in the UW CRB radial forces. While not significant this reduction in load could extend the lifespan of the UW bearings.

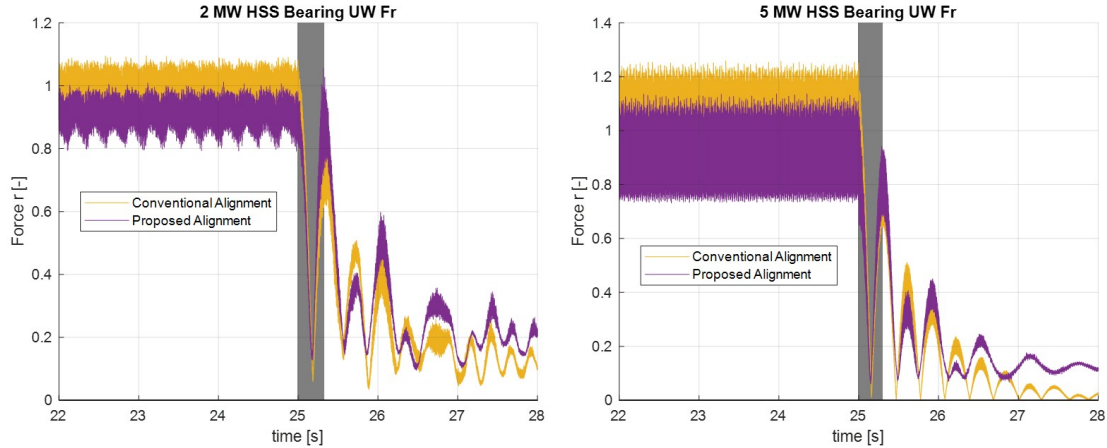


Figure 4.12: Radial loading in 2 MW (left) and 5 MW (right) UW Tapered Roller Bearing during grid interruption event of 2 alignment methods

The main purpose of implementing this dynamic alignment was to improve the response of the bearings during grid interruption events. The loading inside the bearing during the grid interruption event is shaded in gray on each of the previous plots. These forces can also be viewed on a polar plot relating angle and force over the first force reversal as seen in figure 4.13 for the 2 MW model and figure 4.14 for the 5 MW model. The key aspects of each of these polar plots are summarized in table 4.1 for the 2 MW model and table 4.2 for the 5 MW model. It can be seen in table 4.1 that while the overall loading in the DW bearing increased, the desired behavior during grid interruption events was achieved for the 2 MW model. The minimum radial load saw an increase of almost 15% of the steady state radial load, ensuring that skidding would not be a concern. This did come at the cost of a small increase in the change in contact angle of about 6 degrees. The goal of the dynamic alignment method is to reduce both the impact loading and increase the minimal radial load experienced during the grid interruption event. While the impact loading in the DW bearing increased slightly due to an increase in the contact angle, the change is negligible and the benefit of preventing skidding is substantial. The 2 MW UW bearing saw an increase in minimal

radial load of almost 7% while also achieving a minimal reduction in change in contact angle. This reduction is not likely to provide much benefit as the change is small and the loading still changes rapidly over a small period of time, but the increase in minimal radial load is again substantial as the dynamic alignment method never falls below 12.7% of the steady state loading in the bearing likely avoiding cases of skidding.

The 5 MW DW bearing showed all of the effects desired when proposing the dynamic alignment method. The change in contact angle over the grid interruption was reduced by nearly 30 degrees while the minimal radial load saw an increase of approximately 13% of the steady state radial load when compared to the statically aligned case. These two improvements come at the cost of an increased steady state load as previously discussed. The UW bearing sees a 13° in change in contact angle, and the minimum radial load experienced increased by about 5% of the steady state value when compared to the conventional alignment method. This change in reversal amount is still small but could warrant further inspection as the goal is to minimize the impact loading on the bearings. However the minimal radial load experienced by the bearing during the grid interruption in the conventionally aligned case is nearly 0 and the 5% improvement in the loads obtained from dynamic alignment amounts to a substantial reduction in skidding incurred by the bearing

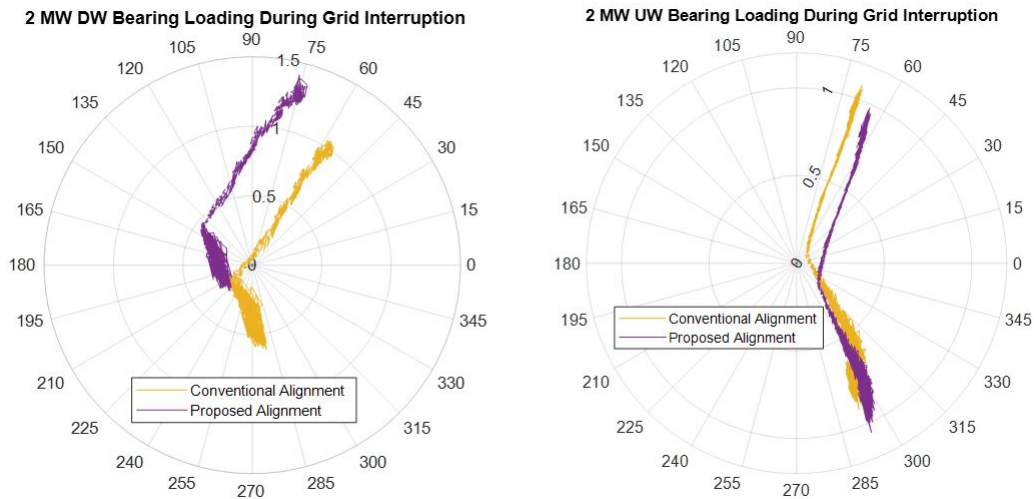


Figure 4.13: Loading Zones in 2 MW HSS Bearings during grid interruption event of 2 alignment methods

Table 4.1: 2 MW model grid interruption transience for conventional and proposed alignments

Model	Test Case	DW Reversal Amount	DW Min Radial Load	DW Max Radial Load	UW Reversal Amount	UW Min Radial Load	UW Max Radial Load
2 MW	Conventional Alignment	146°	.029	1.055	135°	.059	1.081
	Proposed Alignment	152°	.172	1.410	129°	.127	1.056

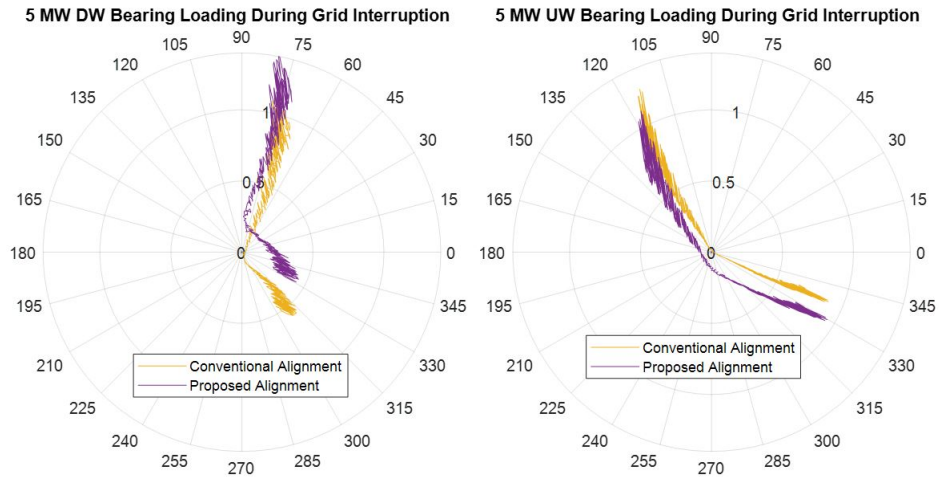


Figure 4.14: Loading Zones in 5 MW HSS Bearings during grid interruption event of 2 alignment methods

4.5 Summary

After previously identifying the potential benefits of NTL on bearing failure modes during grid interruption events a study was performed to determine if the benefits could be replicated by dynamically aligning the HSC using an offset generator. It was shown that adding an additional offset to the generator to align the coupling at full rated power steady state operation was effective for reducing concerns of skidding in the HSS bearings across both 2 MW and 5 MW turbines. The minimal load seen during the grid interruption event was increased substantially in all cases. This was however not without consequence as the new alignment procedure created an increase in the steady state radial load in the DW bearing. This could be a potential cause for concern as the operational loading in the bearing is approximately 30% higher than conventional alignment methods. Additionally, the 2 MW DW and 5 MW UW bearings did not experience a reduction in the change in contact angle as expected. The increase seen in the change in contact was small but could still result in more impact loading in the bearings as the direction the force is being applied changes

Table 4.2: 5 MW model grid interruption transience for conventional and proposed alignments

Model	Test Case	DW Reversal Amount	DW Min Radial Load	DW Max Radial Load	UW Reversal Amount	UW Min Radial Load	UW Max Radial Load
5 MW	Conventional Alignment	124°	.014	1.126	142°	.009	1.251
	Proposed Alignment	95°	.143	1.399	155°	.060	1.110

more rapidly. Overall the increase in impact loading is small in comparison to the improvements made in possible skidding conditions. Skidding continues to be one of the largest causes of bearing failure today as bearings are often being operated at high speeds when grid interruptions occur. The ability to reduce the occurrences of skidding could prove substantial in the improvement of overall lifespan of HSS bearings.

Chapter 5

Conclusions and Discussion

The first objective of this work was to outline the potential uses of various models used for studying electromechanical interaction and then determine a model best fit for studying the impact of NTL on HSS bearing failure modes. It was determined that for electrical modeling isolated component lumped parameter models captured the necessary information for simulating the mechanical interface of the drivetrain to the generator. This allows more complex electrical models to be used in coordination with isolated HSC models to perform detailed electrical analysis. For the purpose of this report, it was determined that the high fidelity full gearbox model was necessary to capture the bearing forces and misalignment necessary for HSS bearing analysis.

After the appropriate model was chosen 2 wind turbine models were used to determine the impact NTL had on potential bearing failure modes. These models were of a 2 MW and a 5 MW wind turbine drivetrain. The 2 models were studied for the impact static NTL had on bearing skidding and impact loading. It was found that applying appropriate NTL could remove potential cases of skidding in the DW TRB seen during grid interruption events. It was also seen that the impact loading could be reduced by applying NTL as well. Implementing this NTL on a turbine in the field could be a potential area of bearing lifespan improvement and yield lower failure rates of bearings in the future. This presented the question of how to apply the NTL to achieve this improvement in bearing health.

Analysis was performed to determine if offsetting the generator could be an appropriate method of implementing the same bearing behavior achieved by applying NTL at the hub. It was found that statically offsetting the generator height could replicate the NTL applied at the hub

connection point to a high degree of accuracy. The next part of the work, investigated the magnitude generator offset to improve HSS bearing health. By implementing a new HSC alignment technique that increases the offset of the generator to take into account torque induced misalignment in the drivetrain, bearing health can be further improved, minimizing the misalignment in the system while adding the NTL necessary to prevent skidding. This new alignment method improved minimal load seen in the HSS bearings for each of the models. The increases in minimal load should lead to decreases in cases of skidding in the HSS bearings, but it comes at the cost of increases in impact loading seen in the 2 MW DW and 5 MW UW bearings. The increase in impact loading are small in comparison to the skidding improvements, but still future study is needed on the potential effects.

5.1 Future Work

The new method of aligning the generator comes with many aspects that need further investigated. The added generator height creates misalignment when the turbine is not running at full power. Future study is needed on how often turbines are operating at or near full power and the impact of the misalignment in the HSC when the turbine is not operation. Additionally, to better study the impact loading in the bearing a more detailed bearing model is required to understand the full behavior of the bearing. The analysis in this report was performed without the full contact geometry of the bearing present. Larger loadings can lead to deformation and other potential failure modes in the HSS bearings. This analysis should be studied further with detailed bearing models present to understand the full effect NTL has on HSS bearing health. Additionally, running the test cases outlined in this report on a full-scale dynamometer like the ones at the Dominion Energy Innovation Center would allow this analysis to be verified for its accuracy.

Bibliography

- [1] Dirk Abel, Christian Brecher, Rik W. de Doncker, Kay Hameyer, Georg Jacobs, Antonello Monti, Wolfgang Schröder, and Andreas Hirt, editors. *Conference for Wind Power Drives, CWD 2019 : Aachen 12th-13th of March : conference proceedings, Aachen, 12th-13th of March 2019; 1. Auflage*, Norderstedt, Mar 2019. 4th Conference for Wind Power Drives, Aachen (Germany), 12 Mar 2019 - 13 Mar 2019, Books on Demand.
- [2] Dassault Systemes Simulia Corp. Simpack documentation, 2020.
- [3] P. Dvorak. What are the functions of couplings and torque limiters in wind turbines? *Windpower Engineering and Development*, 2014.
- [4] P. Dvorak. Extreme torsional loads damage more than wind turbine gearboxes. *Windpower Engineering and Development*, 2016.
- [5] Yi Guo and Jonathan Keller. Investigation of high-speed shaft bearing loads in wind turbine gearboxes through dynamometer testing. *Wind Energy*, 21(2), 11 2017.
- [6] Jonathan A. Keller, Benjamin Gould, and Aaron Greco. Investigation of bearing axial cracking: Benchtop and full-scale test results. 8 2017.
- [7] G. Knitz. A guide to wind turbine alignment. March 2012.
- [8] C. Kraft. How to design your gears. <https://hackaday.com/2010/06/30/how-to-design-your-gears/>, 2010.
- [9] Y. Guo L. Sethuraman, J. Keller and B. McNiff. Gearbox 2 high-speed shaft loads analysis. <https://www.nrel.gov/docs/fy15osti/63870.pdf>, 2015.
- [10] D. Matzke, R. Schelenz, S. Reisch, B. Roscher, G. Jacobs, J. Theling, M. Schroers, C. Löpenhaus, and C. Brecher. Validation of the gearbox load calculation of a wind turbine MBS model. *Journal of Physics: Conference Series*, 1037:062025, jun 2018.
- [11] United States Department of Energy. Wind vision: A new era for wind power in the united states. <https://www.energy.gov/eere/wind/maps/wind-vision>, 2014.
- [12] F Oyague. Gearbox modeling and load simulation of a baseline 750-kw wind turbine using state-of-the-art simulation codes.
- [13] F Oyague. Gearbox reliability collaborative (grc) description and loading. 11 2011.
- [14] S. Sheng. Wind turbine gearbox reliability database, condition monitoring, and operation and maintenance research update. <http://www.nrel.gov/docs/fy16osti/66028.pdf>, 2016.

- [15] K. Smith. What to know when setting two-row tapered roller bearings in wind turbine gearboxes. *Windpower Engineering and Development*, 2020.
- [16] O. Tonks and Q. Wang. The detection of wind turbine shaft misalignment using temperature monitoring. *CIRP journal of manufacturing science and technology.*, 17:71–79, May 2017.
- [17] Turbosquid. Wind generator 002.
<https://www.turbosquid.com/3d-models/3d-wind-turbine-model/755190>, 2013.
- [18] M. Whittle. *Wind Turbine Generator Reliability: An Exploration of the Root Causes of Generator Bearing Failures*. PhD thesis, Durham University., May 2013.
- [19] Caichao Zhu and Yao Li. *Reliability Analysis of Wind Turbines*. 10 2018.